

Spectroscopic and Electrochemical Probes of Electronic Coupling in Some Cyanide-Bridged Transition Metal Donor/Acceptor Complexes

Murielle A. Watzky, Ariel V. Macatangay, Richard A. Van Camp, Selma E. Mazzetto, Xiaoqing Song, John F. Endicott,* and Tione Buranda

The Department of Chemistry, Wayne State University, Detroit, Michigan 48202-3489

Received: June 11, 1997[⊗]

The effects of donor–acceptor (D/A) electronic coupling, H_{DA} , on the spectroscopic and electrochemical properties of several series of CN^- -bridged transition metal complexes have been examined. The complexes employed were formed by ruthenation of $M(L)(CN)_2^{n+}$ parent complexes (for $n = 0$, $M = Ru(II)$ or $Fe(II)$, and $L = bpy$ or $phen$; for $n = 1$, $M = Cr(III)$, $Rh(III)$, or $Co(III)$, and $L = bpy$, $phen$, or a tetraazamacrocyclic ligand). The observed half-wave potentials of the resulting CN^- -bridged D/A complexes spanned a 300–350 mV range in contrast to the range of about 80 mV expected on the basis of the oscillator strength, h_{DA} , of the D/A charge-transfer $MM'CT$ absorption band and the geometrical distance between donor and acceptor, r_{DA} . Different series of complexes exhibit different correlations between $E_{1/2}$ and h_{DA} . Several factors have been found to contribute to these differences: (a) symmetry effects; (b) solvational differences that arise when nonbridging ligands are changed; (c) solvational effects arising from differences in overall electrical charges; (d) partial delocalization of electron density along the D/A axis in such a way as to reduce the effective distance between centers of charge, r_{ge}^c . To take account of the effects of the solvational factors, systematic examination has been made of (a) the metal independent shifts of $E_{1/2}$ which occur when nonbridging ligands are changed; (b) the differences in $E_{1/2}$ that occur in closely related $Ru(III)/Ru(II)$ couples which differ in charge; and (c) solvent perturbations of $E_{1/2}(Ru(NH_3)_5^{3+,2+})$ and solvatochromic shifts of the central metal-to-ligand charge transfer (MLCT) and $MM'CT$ absorbancies of $(bpy)_2(CN)Ru(CNRu(NH_3)_5)^{3+}$ and $(bpy)_2-Ru(CNRu(NH_3)_5)^{6+}$. The experimental observations indicate that changes in the nonbridging ligand of the central metal can result in a range of about 90 mV variation in $E_{1/2}(Ru(NH_3)_5^{3+,2+})$, the effect of a one unit increase in charge of the central metal is to increase $E_{1/2}$ by approximately 65 ± 15 mV, solvent perturbations of $E_{1/2}$ and the electron-transfer reorganizational energy, λ_r , are approximately equal in magnitude, solvational corrections can be treated linearly, and the solvational contributions to $E_{1/2}$ that arise from charge delocalization are less than about 10 mV in these complexes. The complexes have a very rich charge-transfer spectroscopy, and in some complexes as many as seven different CT transitions can be identified which depend on the oxidation state of the $Ru(NH_3)_5$ moiety. There is evidence for considerable mixing between these transitions. The mixed valence ($Ru(NH_3)_5^{2+}/Ru(NH_3)_5^{3+}$), bisruthenates exhibit a unique $Ru(NH_3)_5/M$ $MM'CT$ component in addition to the expected $Ru(NH_3)_5^{2+} \rightarrow Ru(NH_3)_5^{3+}$ CT; this relatively weak absorption tracks the dominant $Ru(NH_3)_5$ /central metal $MM'CT$ absorption, and it is attributable to the different effects of local $M_c(CN^-)Ru(NH_3)_5$ electronic coupling in the mixed valence complex. Values of $E_{1/2}(\text{obsd})$, corrected for solvational effects implied by the experimental observations, correlate with h_{DA} , corrected for symmetry effects, $E_{1/2}(\text{corr}) = E_{1/2}(\text{ref}) \pm (4.2 \times 10^{-4}) h_{DA}/r_{DA}$, only if the “solvational correction” for $Fe(II)$ - and $Ru(II)$ -centered complexes is about 70% larger than suggested by the experimental observations. This may imply greater charge delocalization onto (or from) the bridging ligand for these two metal centers. For either interpretation, the correlation between $E_{1/2}(\text{obsd})$ and h_{DA} implies that $r_{ge}^c \leq 0.62r_{DA}$. This relatively small value of r_{ge}^c can be interpreted in terms of charge delocalization onto (or from) the bridging ligand, and it can be qualitatively described in terms of perturbational mixing of the ground and excited electron-transfer states with higher energy CT states. This mixing is described in terms of a multicenter ($M_c-C-N-Ru_c$) vibronic coupling model which was previously (*Inorg. Chem.* **1996**, *34*, 3463) used to account for the anomalous shifts of the CN^- stretch in CN^- -bridged D/A complexes.

Donor–acceptor (D/A) systems, and the related electron-transfer processes, are of central importance in chemistry.¹ Such systems have been extensively studied experimentally^{1–24} and theoretically,^{1–4,13,17,25–37} but a number of fundamental issues remain unresolved. Among these are various aspects of the electronic coupling between donors and acceptors in electron-transfer systems.^{4,5–10,19–22,26–36,38} We have recently been examining the effects of strong D/A electronic coupling on the properties of covalently linked transition metal (D/A) com-

plexes.^{37,39} The results of our observations have led us to consider the applicability of “vibronic” models in which the electronic coupling matrix element, H_{DA} , is a function of some of the nuclear coordinates involved in the electron-transfer process.^{28,32–35,40} In the present paper we describe our spectroscopic and electrochemical observations on several series of cyanide-bridged, transition metal D/A complexes, and we compare these observations to expectations based on a simple, semiclassical vibronic model.

Electron-transfer kinetics of D/A systems are usually analyzed in terms of the product of functions of an electronic factor (e.g.,

[⊗] Abstract published in *Advance ACS Abstracts*, October 15, 1997.

the electronic matrix element H_{DA}) and a nuclear reorganizational factor (λ_r); for example in the semiclassical limit the electron-transfer rate constant can be represented as in eq 1, in

$$k_{et} = \kappa_{el}\kappa_{nu}\nu_{nu} \quad (1)$$

which κ_i ($i = el$ for electronic; $i = nu$ for nuclear) are transmission coefficients, and ν_{nu} is the correlated nuclear frequency at the transition state. Very clearly, related parameters govern a D/A charge transfer (DACT) absorption: the absorption band maximum can be correlated with the transition-state energy,³ the oscillator strength is proportional to H_{DA}^2 ,^{2,23} and the square of the bandwidth is correlated with λ_r .^{3,40} While the contributions of nuclear reorganizational factors to electron-transfer rates and to CT absorption bandwidths have been well documented,^{1,5-7,10-14,17,42} the magnitudes and the origins of the contributions of electronic factors have often been difficult to define and difficult to directly investigate experimentally and the experimental observations have sometimes been subject to conflicting interpretations.^{19-21,26-36,39,40,43-52} More specifically, it has been difficult to establish how (and, sometimes, whether) the components of the spatial region between donor and acceptor contribute to the magnitude of the electronic factor.^{1-12,16,30} It has been comparably difficult to establish how and to what extent D/A electronic coupling modifies the properties of the ground state,^{2-7,19-22,24,26,28-30,32-36} and the relationship between the observed variations in ground-state properties and H_{DA} has also been difficult to establish.^{28,29,39,44-52}

For some time we have had an interest in the use of the CT perturbations of neighboring groups to enhance the electronic coupling of electron-transfer donors and acceptors.^{8,39-41,43} The present report describes some studies of CT perturbations of D/A coupling in CN⁻-bridged, transition metal D/A complexes. We have examined the spectroscopic manifestations of electronic coupling in several series of CN⁻-bridged complexes, and we have compared the spectroscopic information to electrochemical measures of the trends in ground-state stabilization energies. The observations seem to be consistent with a model^{40,41} in which there is synergistic coupling between the electron-transfer states and higher energy donor-to-CN⁻ and CN⁻-to-acceptor CT excited states.

Experimental Section

Syntheses of most of the compounds used in this study have been reported previously.^{39,40} Syntheses are also described elsewhere for the complexes $M(ms\text{-}Me_6[14]aneN_4)(CN)_2^{2+}$ ($M = Cr^{3+}$,⁵⁴ Rh^{3+} ,⁵⁵ and Co^{3+} ⁵⁶); $M(rac\text{-}Me_6[14]aneN_4)(CN)_2^{2+}$ ($M = Cr^{3+}$ ⁵⁴ and Rh^{3+} ⁵⁵); $Cr([15]aneN_4)(CN)_2^{2+}$,⁵⁴ $M([15]aneN_4)Cl_2^{2+}$ ($M = Rh^{3+}$ ⁵⁷ and Co^{3+} ⁵⁸); and $M(NH_3)_5CN^{2+}$ ($M = Cr^{3+}$ ⁵⁹ and $M = Rh^{3+}$ ⁶⁰). Minor variations of these procedures were used for the compounds reported here. Elemental analyses and spectroscopic properties of the compounds synthesized were in good agreement with expectation and with literature reports. Ruthenation of the cyano complexes employed procedures described previously.^{39,40,61} The ruthenated complexes were characterized by their visible-UV and IR spectroscopy, redox titrations, and elemental and inductively coupled plasma (ICP) analysis. The ruthenated complexes were prepared in small amounts, and fresh preparations were used in most experiments. We did observe that the ruthenates of the Cr(III)-centered cyano complexes could be stored as solids (in an Ar atmosphere) in a refrigerator for a few months without evidence of decomposition. Additional details of the synthesis and characterization of these am(m)ine complexes are to be published elsewhere.⁶²

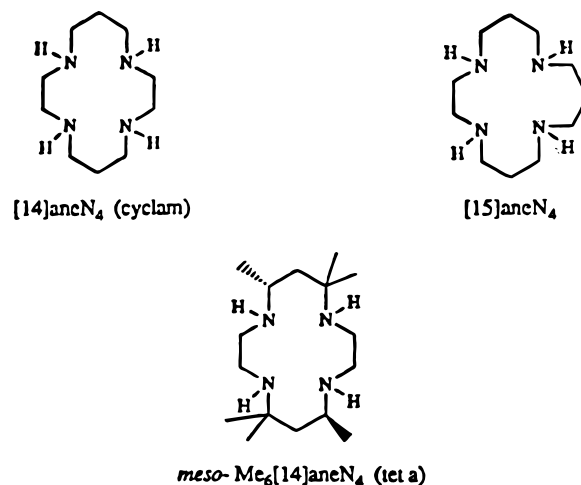


Figure 1. Macrocyclic nonbridging ligands used in this study. For proper names see ref 53.

Cyclic Voltammetry. The apparatus has been described elsewhere.^{39,40} Redox potentials were measured from solutions in 0.1 M TEAP (or 0.1 M TBAH)/acetonitrile at a scan rate of 500 mV/s. A platinum disk working electrode, previously polished with 0.3–0.05 μm Buehler alumina suspension, a platinum wire counter electrode, and an Ag/AgCl reference electrode were used. Ferrocene or diacetylferrocene (0.367 and 0.827 V vs SCE, respectively)⁶³ was dissolved in the sample solution and taken as an internal standard. The potential values were averaged over 5–10 determinations; standard deviations were typically ± 3 mV. A solid sample of $(bpy)_2Ru(CNRu(NH_3)_5)(LAS)_6$ ($LAS =$ lasalocid) was obtained by adding a 3-fold excess of Na_3LAS (Aldrich Chemical Co.) to a methanolic solution of the ruthenium complex and then allowing the solvent to evaporate. This solid was dissolved in 0.1 M TEAP/ CH_3CN solutions for the electrochemical measurements.

Absorption Spectroscopy. Spectra were collected using either an HP-8452 diode array spectrophotometer or on an OLIS modified Cary-14 spectrophotometer. Spectral deconvolution was performed with Spectracalc software from Galactic Inc. (example in Figure 1s). Anaerobic solutions of $Ru(NH_3)_5^{2+}$ metalates were made either by dissolving the metalate in Ar-degassed water (freeze-pump-thaw cycles) or by reducing the $Ru(NH_3)_5^{3+}$ metalate (for $M_c = Fe(II)$ or $Ru(II)$ only) in water on Zn(Hg) with an Ar purge and transferring the solution anaerobically to a cuvette fused to the purging vessel. Molar absorptivities were determined by redox titrations: a deaerated aliquot of a standard solution of Ce^{4+} (0.1 M $(NH_4)_2Ce(NO_3)_6$ in 1 M CF_3SO_3H) or $Fe(H_2O)_6^{3+}$ (0.1 M $Fe(NO_3)_3$ in 1 M CF_3SO_3H) was added by means of a syringe to the sample solution in the purging apparatus, and the spectrum was recorded after each addition. The original spectrum could be regenerated by addition of $Ru(NH_3)_6^{2+}$ to the solution, and some samples were back-titrated with standard solutions of $Ru(NH_3)_6^{2+}$ (0.05 M $Ru(NH_3)_6Cl_3$ in H_2O). Molar absorptivities were determined from plots of absorbance vs concentration of added oxidant (or reductant) (example in Figure 2s). Solutions of $(bpy)_2Ru(CNRu(NH_3)_5)_2(LAS)_6$ in methanol were obtained by adding Na_3LAS in about 3-fold stoichiometric excess to a solution of the $(bpy)_2Ru(CNRu(NH_3)_5)_2^{6+}$ complex ($\sim 10^{-4}$ M) and allowing the mixture to equilibrate for several hours.

Results

Some important general features of the ruthenated complexes have been described previously.^{39,40,61,64} Since many of these compounds are of moderate to marginal stability, we have been

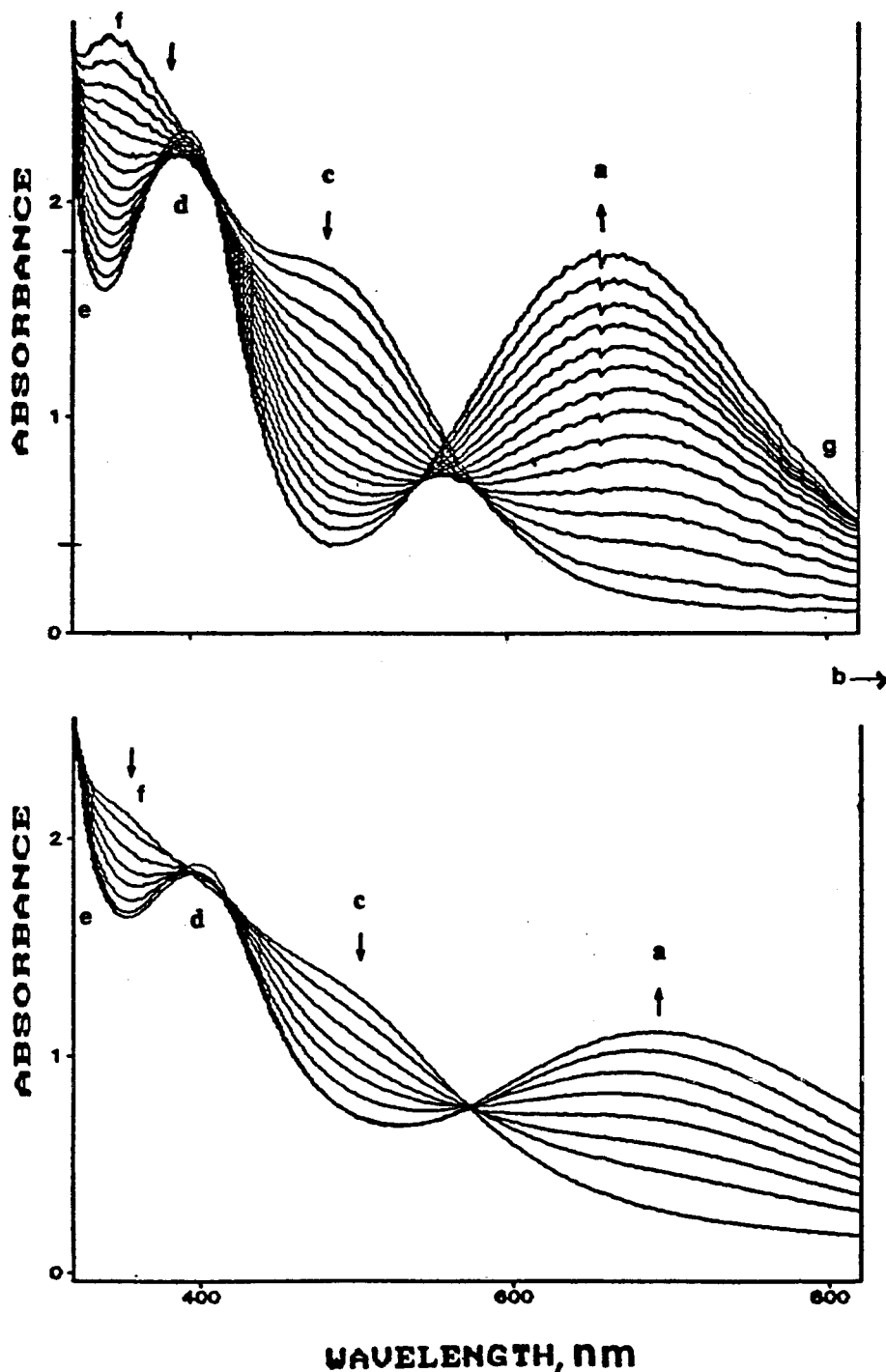


Figure 2. Spectroscopic changes during the Fe³⁺ oxidation of (bpy)₂Ru(CNRu(NH₃)₅)₂⁴⁺ (top) and (bpy)₂(CN)Ru(CNRu(NH₃)₅)₂²⁺ (bottom). The standard Fe³⁺ solution was added in microliter aliquots to a 3 mL sample in a cuvette (all deaerated). CT absorption assignments are (a) Ru(bpy)₂²⁺ → Ru(NH₃)₅³⁺; (b) Ru(NH₃)₅²⁺ → Ru(NH₃)₅³⁺; (c) Ru(NH₃)₅²⁺ → bpy; (d) Ru(bpy)₂²⁺ → bpy; (e) CN⁻ → Ru(NH₃)₅³⁺; (f) Ru(NH₃)₅²⁺ → CN⁻.

careful to prepare samples of the least stable compounds on the same day that they were used, and we have routinely compared IR and vis-UV spectra and CV behavior of each preparation with similar measurements reported elsewhere.^{39,40,61,63}

A. CT Absorption Spectra. 1. Classification. The ruthenated polypyridyl complexes exhibit a rich charge-transfer spectroscopy, with several metal-oxidation state dependent, near IR to near UV absorptions. These bands can be characterized by their behavior in the redox titrations (see Figures 2–4, 2s, and 3s⁶⁵). The important CT absorption bands are as follows:

(a) The first are the Ru(NH₃)₅/central metal CT absorptions. These varied in intensity ($\epsilon_{\max} = (0-5) \times 10^3 \text{ M}^{-1} \text{ cm}^{-1}/\text{Ru}$) and energy ($\lambda_{\max} = 340-950 \text{ nm}$) depending on the central

metal. The characteristics of some of these absorption bands are summarized in Table 1; others can be found elsewhere^{39,40} (see Table 1s).⁶⁵ These bands are usually nearly Gaussian in contrast to the analogous bands reported for (NC)₅Os-CNRu(NH₃)₅^{-66,67}

(b) During the course of the redox titrations of the bisruthenates a weak absorption ($\epsilon_{\max} \gg 10^2$) developed in the near IR (800–1000 nm). The intensity of this absorption maximized when sufficient oxidant had been added to generate a 1:1 ratio of Ru(NH₃)₅²⁺ to Ru(NH₃)₅³⁺. This band was almost always convoluted with the more intense MM'CT transition, and the absorptions in this spectral region were sometimes complicated by impurity absorptions.⁶⁸ This is clearly a Ru(NH₃)₅²⁺ → Ru-

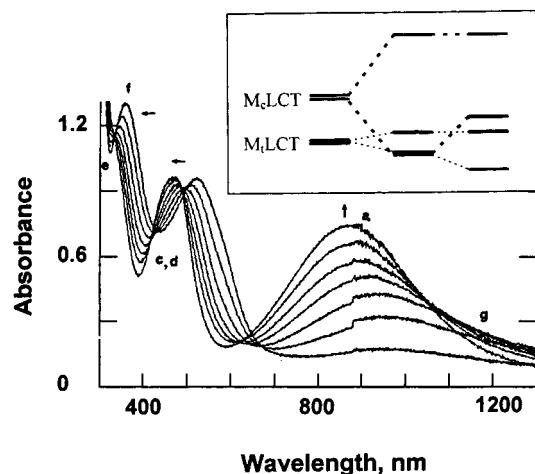


Figure 3. Spectroscopic changes during the Fe^{3+} oxidation of $(\text{bpy})_2\text{-Fe}(\text{CNRu}(\text{NH}_3)_5)_2^{4+}$. See Caption of Figure 2 and text for assignments and details. Inset illustrates the effect of MLCT and $M'LCT$ mixing when components of the same symmetry are very similar in energy. For simplicity only two components (symmetric and antisymmetric)^{79,80} are shown for these CT transitions of the two metals.

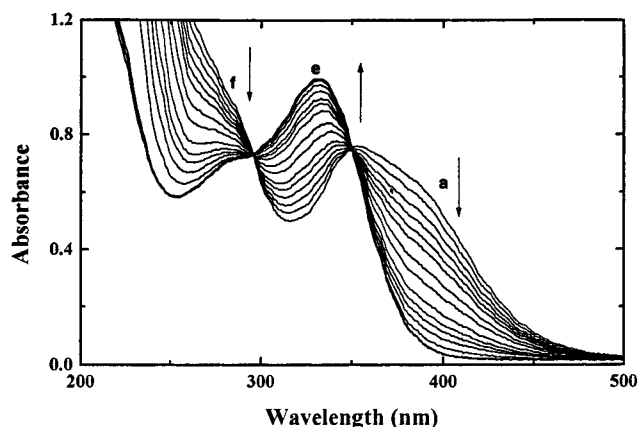


Figure 4. Spectroscopic changes during the Fe^{3+} oxidation of $(\text{H}_3\text{N})_5\text{-Rh}(\text{CNRu}(\text{NH}_3)_5)_2^{4+}$. See caption of Figure 2 and text for assignments and details.

$(\text{NH}_3)_5^{3+}$ CT transition. The behavior of these absorptions in the $\text{M}(\text{MCL})(\text{CNRu}(\text{NH}_3)_5)_2^{5+}$ complexes will be discussed in detail elsewhere.⁶² Owing to the much greater overlap of these weak absorptions with the visible range of CT absorptions, we have not attempted to systematically deconvolute them from the spectra of the polypyridyl complexes.

(c) Absorption bands of intermediate intensity occur in the 350–500 nm region of all polypyridyl complexes containing $\text{Ru}(\text{NH}_3)_5^{2+}$. Comparable transitions do not occur when the central metal has saturated ligands such as in the $(\text{MCL})\text{M}(\text{CNRu}(\text{NH}_3)_5)_2^{5+}$ complexes in which $\text{M} = \text{Rh}(\text{III})$, $\text{Co}(\text{III})$, or $\text{Cr}(\text{III})$ (compare Figures 2 and 3s;⁶⁵ skeletal structures of MCL ligands in Figure 1). This supports the previous assignment⁶¹ of these transitions as $\text{Ru}(\text{NH}_3)_5^{2+} \rightarrow$ polypyridyl $M_L\text{LCT}$ transitions. These absorptions are almost always convoluted with $\text{MM}'\text{CT}$ transitions or with central metal to polypyridine CT transitions. The most striking examples of this occur for the $(\text{Ru}$ and $\text{Fe})\text{(PP)}(\text{CNRu}(\text{NH}_3)_5)_2^{4+}$ complexes in which the $\text{Ru}(\text{NH}_3)_5^{2+} \rightarrow \text{PP}$ transitions are evidently mixed with the $\text{M}(\text{PP})_2^{2+}$ MLCT transitions (see especially Figures 2 and 3 and the discussion below). These absorptions are summarized in Table 2.

(d) For the complexes with $\text{Ru}(\text{bpy})_2^{2+}$ or $\text{Fe}(\text{bpy}$ or $\text{phen})_2^{2+}$ centers, a central metal to bpy $M_c\text{LCT}$ transition is observed ($\lambda_{\text{max}} = 400\text{--}560$ nm).

(e and f) A relatively weak band can often be resolved at about 340 nm in the CN^- -bridged complexes containing $\text{Ru}(\text{NH}_3)_5^{3+}$, while a band of roughly comparable intensity is almost always observed in the 350–400 nm spectral region in the CN^- -bridged complexes containing $\text{Ru}(\text{NH}_3)_5^{2+}$. These absorptions are assigned as $\text{CN}^-(\pi) \rightarrow \text{Ru}(\text{III})$ and $\text{Ru}(\text{II}) \rightarrow \text{CN}^-(\pi^*)$, respectively, and they are summarized in Table 3. This assignment is consistent with the occurrence in comparable spectral regions of MLCT absorption bands in $\text{Ru}(\text{CN})_6^{4-}$ and LMCT absorption bands in $\text{Ru}(\text{CN})_6^{3-}$.^{69–71}

(g) A relatively weak absorption always occurs in the mixed valence, $\text{Ru}(\text{NH}_3)_5^{3+}/\text{Ru}(\text{NH}_3)_5^{2+}$, bisruthenates at 3500–5000 cm^{-1} lower energy than the $\text{MM}'\text{CT}$ absorption maximum (see Figures 2, 3, and 3s). These absorptions do not appear in any of the monoruthenates. A relatively simple interpretation of this absorption of the half-oxidized complexes is that it is an $\text{MM}'\text{CT}$ transition which involves a central metal orbital which is not directly involved in local Ru_t/M_c D/A coupling. The multicenter, $M_c(\text{CN}^-)\text{-Ru}_t$, D/A coupling argument proposed previously for the symmetrical limit⁴⁰ can be qualitatively generalized to provide a reasonable basis for this assignment (see Figures 7 and 4s,⁶⁵ and the discussion below). This issue is being further examined.⁶²

The spectra of the cyano ruthenates of the $\text{M}(\text{MCL})(\text{CN})_2^+$ complexes contain the CT bands a, b, e, f, and g, but they do not contain the visible region MLCT bands so characteristic of their polypyridyl analogues.

The transitions are assigned to the above categories (designated by a–g) for $(\text{bpy})_2\text{Ru}(\text{CNRu}(\text{NH}_3)_5)_2^{n+}$ in Figure 2.

These assignments are based on (1) the behavior of the designated absorption during a redox titration; (2) the comparison of absorption spectra of several complexes; and (3) literature precedents.

2. *The $\text{Ru}^{\text{II}} \rightarrow \text{CN}^-(\pi^*)$, MLCT, and $\text{CN}^-(\pi) \rightarrow \text{Ru}(\text{III})$, LMCT, Absorptions.* The CN^- -based LMCT and MLCT transitions have turned out to be relatively important to the interpretation of trends found in this study, so a few additional comments about these assignments are in order. The charge-transfer spectra of $\text{M}(\text{CN})_6^{3-}$ and $\text{M}(\text{CN})_6^{4-}$ complexes have been examined, and several LMCT and MLCT transitions have been assigned.^{69–71} The complexes with $\text{M} = \text{Fe}$ or Ru are of particular interest in the present context. Since several symmetry-adapted ligand orbital combinations must contribute to the spectra and M-CN bonding in the O_h complexes,^{69–71} quantitative comparisons are a little difficult. For our purposes it is useful to note that the MLCT transitions ($\text{Ru}^{\text{II}}t_{2g} \rightarrow t_{1u}$ or t_{2u}) tend to occur at higher energy ($\Delta h\nu_{\text{max}} \geq 2 \times 10^3 \text{ cm}^{-1}$), while the $\text{CN}^- \rightarrow \text{M}(\text{III})$ CT transitions ($t_{2u} \rightarrow \text{Ru}^{\text{III}}t_{2g}$) occur at lower energy ($\Delta h\nu_{\text{max}} \approx 4.8 \times 10^3 \text{ cm}^{-1}$) for Ru than for Fe . This is the ordering one would predict based on the respective $\text{M}(\text{CN})_6^{3-}$ redox potentials ($E_{1/2}(\text{Ru}) - E_{1/2}(\text{Fe}) \approx 0.5 \text{ V}$);⁶³ in fact the observed differences in MLCT and LMCT energies compare favorably with the expectation of $4 \times 10^3 \text{ cm}^{-1}$ for this difference based only on the differences in redox potentials.

Related reasoning would lead one to expect a CN^- - $\text{Ru}(\text{III})$ LMCT transition at about $33 \times 10^3 \text{ cm}^{-1}$ in a $\text{Ru}(\text{NH}_3)_5\text{CN}^{2+}$ complex in which $E_{1/2}(\text{Ru}^{3+,2+}) \approx 0.3 \text{ V}$. Thus, the absorptions observed at $(30 \pm 3) \times 10^3 \text{ cm}^{-1}$ in the $\text{MCNRu}(\text{III})$ complexes are very consistent with this simple argument (for example, it neglects any differences in reorganizational energies) and the $\text{CN}^-(\pi) \rightarrow \text{Ru}(\text{III})$ assignment.^{69–73} The same reasoning applied to the bands assigned as $\text{Ru}(\text{II}) \rightarrow \text{CN}^-(\pi^*)$ MLCT absorptions in Table 3 suggests that the lowest energy absorption band should occur at $\sim 40 \times 10^3 \text{ cm}^{-1}$,⁷² rather than the $(27 \pm 3) \times 10^3 \text{ cm}^{-1}$, which we observe. However, the $\text{Ru}(\text{CN})_6^{3-}$

TABLE 1: MM'CT Absorption Bands and Half-Wave Potentials of Some (L)(M(CNRu(NH₃)₅)₂)ⁿ⁺ and (L)(CN)M(CNRu(NH₃)₅)ⁿ⁺ Complexes

M	L ^a	n	formal charges of metals (Ru, M, Ru)	MM'CT λ _{max} , nm (ε _{max} /10 ³ , M ⁻¹ cm ⁻¹) [Δν _{1/2} /10 ³ , cm ⁻¹] in H ₂ O ^b	E _{1/2} (Ru(NH ₃) ₅) ^{3+,2+} ^c V(ΔE _p in mV) in CH ₃ CN
Rh(III)	<i>t</i> -[14]aneN ₄	5	(2,3,2)	{342(0.8)[6.0]} ^d	0.037
Rh(III)	<i>t</i> -Me ₆ [14]aneN ₄	5	(2,3,2)	{338} ^d	0.312 ± 0.007(128)
Rh(III)	<i>t</i> -[15]aneN ₄	5	(2,3,2)	{340} ^d	0.318 ± 0.006(130)
Rh(III)	(NH ₃) ₅	4	(2,3)	{391(655)[6.4]} ^d	0.285 ± 0.006(88)
			(2,3)	{391(655)[6.4]} ^d	
Co(III)	[14]aneN ₄	5	(2,3,2)	501(1.03)[7.0]	0.267 ± 0.006
Co(III)	<i>t</i> -Me ₆ [14]aneN ₄	5	(2,3,2)	513(1.4)[6.0]	0.335 ± 0.003(124)
Co(III)	<i>t</i> -[15]aneN ₄	5	(2,3,2)	{518(0.64)[6.0]}	0.268 ± 0.006(110)
Cr(III)	<i>t</i> -[14]aneN ₄	5	(2,3,2)	500(8.0)[4.9]	0.321 ± 0.000(120)
Cr(III)	<i>t</i> -Me ₆ [14]aneN ₄	5	(2,3,2)	515(6.4)[5.2]	0.364 ± 0.004(121)
Cr(III)	<i>t</i> -[15]aneN ₄	5	(2,3,2)	515(7.1)[4.6]	0.328 ± 0.006(124)
Cr(III)	(NH ₃) ₅	4	(2,3)	462(3.1)[5.7]	0.372 ± 0.003(69)
Cr(III)	<i>t</i> -[14]aneN ₄	3	(2,3)	498(4.4)[5.2]	0.328 ± 0.006(82)

^a See ref 53 for proper names of ligands. ^b ε_{max} determined by redox titration with standard Ce(IV) or Fe(III) solutions (1.0 M in 1 M CF₃SO₃H); nr = not resolved. ^c In 0.1 M TEAP/CH₃CN. Pt disk electrode. Ferrocene (0.367 V vs SSCE) or diacetylferrocene (0.827 V vs SSCE) standards. Average of 3–5 determinations; standard deviations = ±3. Related couples in (CH₃CN): Ru(bpy)₂(CN)₂⁺⁰. ^d There may be significant Ru(II)/CN⁻ MLCT contribution to this absorption.

TABLE 2: Higher Energy CT Absorptions in (bpy)₂M(CNRu(NH₃)₅)₂ⁿ⁺ Complexes

M	n	formal charges of metals (Ru, M, Ru)	probable assignment ^a			
			Ru(II)/bpy (c)	M _c (II)/bpy (d)	Ru _i (II)/CN ⁻ (e)	CN ⁻ /Ru _i (III) (f)
Ru(II)	4	(2,2,2)	20.6(∼9)[∼6]	24.5(10.7)[4.4]	27.4(∼10)[5]	
Ru(II)	6	(3,2,3)	{18(∼2)[27]} ^b	24.9(10.7)[5.1]		∼28(∼5)[4.5]
Fe(II)	4	(2,2,2)	{22(∼5)[5]} ^c	18(∼7)[4.4]	30(∼6)[4.4]	
			26(∼10)[5]			
Fe(II)	6	(3,2,3)		24(∼7)[5]		∼28(∼7)[5]
Rh(III)	5	(2,3,2)	{21(1.5)[5.9]} ^c		{28(2.2)[4.5]} ^d	
			{24.5(2.6)[6]} ^c			
Cr(III)	5	(2,3,2)	{21.6(1.1)[5.8]} ^c		29.8(5.6)[3.8]	
			25.5(1.7)[5.1]			
Cr(III)	7	(3,3,3)			{24.8(0.8)[4.7]} ^e	29.2(5)[4.9]

^a Absorption maxima in cm⁻¹/10³ (ε_{max}, M⁻¹ cm⁻¹) [(Δν_{1/2}, cm⁻¹/10³). Letters in parentheses refer to bands so designated in Figure 2. The most ambiguous assignments or bands which must be of other parentage are indicated with curly brackets. ^b This band may be an artifact of the spectral deconvolution since it lies between the much more intense MM'CT and MLCT absorptions; see Figure 2. It could also be a triplet MLCT, partly allowed by magnetic coupling to the terminal Ru(NH₃)₅³⁺ moieties. ^c Possibly a deconvolution artifact; possibly a second Ru(NH₃)₅²⁺/bpy MLCT component (expected in C_{2v} symmetry), or a higher energy MM'CT component (see Figure 5). ^d This absorption is most likely a MM'CT contribution; see Table 1. ^e The parent Cr(bpy)₂(CN)₂⁺ complex exhibits moderately intense absorptions in this region (hν_{max} = 23.8 × 10³ cm⁻¹, ε_{max} = 362 cm⁻¹ M⁻¹; hν_{max} = 25.3 × 10³ cm⁻¹, ε_{max} = 519 cm⁻¹ M⁻¹) which have been assigned as internal ligand 1π → 3π* transitions partially allowed owing to magnetic coupling to Cr(III). The Co(MCL)(CNRu(NH₃)₅)₂⁵⁺ complexes also exhibit absorptions in this region (hν_{max} ≈ 26 × 10³ cm⁻¹; ε_{max} ≈ 10³ cm⁻¹ M⁻¹).

TABLE 3: Higher Energy CT Absorptions in (MCL)M(CNRu(NH₃)₅)₂ⁿ⁺ Complexes

M	n	MCL ^b	geometry	formal charges of metals (Ru, M, Ru)	probable assignment ^a	
					Ru(II)/CN ⁻ (e)	CN ⁻ /Ru _i (III) (f)
Rh(III)	5	[14]aneN ₄	trans	(2,3,2)	{29.2(0.8)[6.0]} ^c	
Rh(III)	7	[14]aneN ₄	trans	(3,3,3)		30.8(0.4)[6]
Rh(III)	5	<i>m</i> -Me ₆ [14]aneN ₄	trans	(2,3,2)	{29.6(0.9)[5.9]} ^c	
Rh(III)	7	<i>m</i> -Me ₆ [14]aneN ₄	trans	(3,3,3)		
Rh(III)	4	(NH ₃) ₅		(2,3)	{36.4(0.41)7.2]} ^c	
Rh(III)	5	(NH ₃) ₅		(2,3)		30.9(185)[6.7]
Co(III)	5	[14]aneN ₄	trans	(2,3,2)	27.5(0.5)[∼6]	
Co(III)	7	[14]aneN ₄	trans	(3,3,3)		∼27(0.5)[∼6]
Co(III)	5	<i>m</i> -MeMe ₆ [14]aneN ₄	trans	(2,3,2)	26.7(0.4)	
Co(III)	7	<i>m</i> -MeMe ₆ [14]aneN ₄	trans	(3,3,3)		27(0.9)
Cr(III)	5	[14]aneN ₄	trans	(2,3,2)	28.9(0.8)[∼6]	
Cr(III)	7	[14]aneN ₄	trans	(3,3,3)		33.6(3.0)[∼6]
Cr(III)	5	<i>m</i> -MeMe ₆ [14]aneN ₄	trans	(2,3,2)	29.2(1.5)[∼6]	
Cr(III)	7	<i>m</i> -MeMe ₆ [14]aneN ₄	trans	(3,3,3)		33.0(3.1)[∼6]

^a See note a of Table 2. ^b See Figure 1 and ref 53 for structures and formal names. ^c This absorption may contain a MM'CT contribution; see Table 1.

comparison is at best a qualitative one for the (LMCN⁺)–Ru(III) or (LMCN⁺)–Ru(II) systems since it does not take into account the differences that occur when CN⁻ bridges two metals or when the donor atom (N or C) is changed. The comparison

does identify the near UV as the spectral region in which these absorptions are expected to occur. We have used the variations in absorption spectra with the oxidation state of the Ru(NH₃)₅ moiety as the principle basis for our assignments.

TABLE 4: Solvent-Induced Variations in the MM'CT and MLCT Spectra and the Half-Wave Potentials of (bpy)₂(CN)Ru(CNRu(NH₃)₅)₂³⁺ and of (bpy)₂Ru(CNRu(NH₃)₅)₂⁶⁺

complex ^a	property	solvent					
		acetone	acetonitrile	benzonitrile	DMF	DMSO	water
Ru(CNRu) ³⁺	$h\nu_{\max}$ (MM'CT), cm ⁻¹ /10 ³	14.0	13.3	13.5	15.0	15.1	14.3
	$h\nu_{\max}$ (MLCT), ^b cm ⁻¹ /10 ³	22.2		23.4	22.4	22.4	25.0
	$\Delta E_{1/2}$, V	0.54	0.390		0.66	0.72	0.487
Ru(CNRu) ₂ ⁶⁺	$h\nu_{\max}$ (MM'CT), cm ⁻¹ /10 ³	15.2	14.5	14.4	16.6	16.5	15.3
	$h\nu_{\max}$ (MLCT), cm ⁻¹ /10 ³	24.8		25.3	23.6	23.7	25.3
	$\Delta E_{1/2}$, V	0.54	0.404	0.49	0.63	0.66	0.462

^a Abbreviations: Ru(CNRu)³⁺ = (bpy)₂(CN)Ru(CNRu(NH₃)₅)₂³⁺; Ru(CNRu)₂⁶⁺ = (bpy)₂Ru(CNRu(NH₃)₅)₂⁶⁺. ^b Central Ru(II) to bpy MLCT. ^c $\Delta E_{1/2} = E_{1/2}(\text{Fe}(\text{Cp})_2^{+0}) - E_{1/2}(\text{Ru}(\text{NH}_3)_5^{3+,2+})$.

3. *Possible Ru(II) → Rh(III) MM'CT Absorptions.* Assignment of the absorptions at $(29.4 \pm 0.2) \times 10^3 \text{ cm}^{-1}$ in the Rh^{III}-(MCL)(CNRu^{II}(NH₃)₅)₂⁵⁺ complexes is not as straightforward as the preceding discussion might suggest. This can be illustrated by considering the I⁻ → M(III) LMCT absorption in Co(NH₃)₅I²⁺ and Rh(NH₃)₅I²⁺. The σ and π (p orbital symmetries at I⁻) components of these transitions occur at 35.1×10^3 ($\epsilon_{\max} = 16\,000 \text{ cm}^{-1} \text{ M}^{-1}$) and $27 \times 10^3 \text{ cm}^{-1}$ ($\epsilon_{\max} \approx 2700 \text{ cm}^{-1} \text{ M}^{-1}$), respectively for Co, and at 44.2×10^3 ($\epsilon_{\max} = 20\,000 \text{ cm}^{-1} \text{ M}^{-1}$) and $36 \times 10^3 \text{ cm}^{-1}$ ($\epsilon_{\max} \approx 3600 \text{ cm}^{-1} \text{ M}^{-1}$), respectively, for the Rh complex.⁷⁰ On the basis of this comparison one expects "LMCT" absorptions of Rh(III) to be about $9 \times 10^3 \text{ cm}^{-1}$ higher in energy than those of the corresponding Co(III) complex. Since the Ru(II) → Co(III) MM'CT absorption is at $20 \times 10^3 \text{ cm}^{-1}$ in Co([14]aneN₄)-(CNRu(NH₃)₅)₂⁵⁺, the preceding comparison of LMCT spectra suggests that the corresponding absorption of the Rh(III) analogue should occur at $\sim 29 \times 10^3 \text{ cm}^{-1}$. This comparison originally led us to make such an assignment.^{39a} After examining a large number of complexes in which the Ru(II) → CN⁻(π^*) absorption occurs at about this energy, we conclude that a definitive simple assignment is not possible; in fact one would expect that the observed absorption band involves some mixture of these potential chromophores. It is interesting that the Rh(III)-centered complexes have the smallest absorptivities of any of the complexes in this region (the reverse of the observations on LMCT spectra mentioned above). In our discussions below we will take account of the ambiguity in assignment of the MM'CT spectra of Rh(III)-centered complexes by considering both extreme possibilities: (a) that the $29 \times 10^3 \text{ cm}^{-1}$ absorption contains no MM'CT contribution; and (b) that the $29 \times 10^3 \text{ cm}^{-1}$ absorption contains only MM'CT absorption components. However, we will tentatively assign the lowest energy CT absorption in these Rh(III)-centered complexes as Ru(II) → Rh(III) MM'CT. This assignment is supported by observations on the (H₃N)₅Rh(CNRu(NH₃)₅)⁴⁺ complex (Figure 4). This complex exhibits 3–4 collections of absorption bands which depend on the oxidation state of the Ru(NH₃)₅ moiety: (i) bands in the 340–450 nm region which we assign as Ru(II) → Rh(III) CT; (ii) bands in 280–355 nm region which we assign as CN⁻ → Ru(III) CT; (iii) absorptions in the 240–290 nm region which we assign as Ru(II) → CN⁻ CT. The $\sim 5 \times 10^3 \text{ cm}^{-1}$ higher energy of the latter absorptions is consistent with the splittings expected of strongly coupled, nearly isoenergetic Ru(II) → CN⁻ and Ru(II) → Rh(III) transitions. There are higher energy transitions in this complex which we tentatively assign as Ru(NH₃)₅²⁺ → solvent CT.

4. *The Effect of Solvent on the CT Absorptions.* The MLCT (d) and MM'CT (a) absorption bands of (bpy)₂Ru(CNRu(NH₃)₅)₂⁶⁺ shift to 410 and 615 nm, respectively, in methanolic solutions containing a 3-fold stoichiometric excess of Na₃LAS. The LAS³⁻ anion effectively sequesters the ammine complex moieties.⁷⁴ This results in shifts of both the MM'CT and MLCT

absorption bands, which can be interpreted in terms of a change of solvent environment. The MLCT and MM'CT bands shift in opposite directions with respect to the respective 395 and 700 nm absorptions of (bpy)₂Ru(CNRu(NH₃)₅)₂⁶⁺ in water. Different shifts of the MLCT and MM'CT absorptions are a characteristic feature of this complex in many solvents (Table 4). In many of the solvents employed we have been able to obtain half-wave potentials for the Ru(NH₃)₅^{3+,2+} couple (referenced to Fe(Cp)₂⁺⁰) and in most instances the related information for the (bpy)₂(CN)Ru(CNRu(NH₃)₅)³⁺ complex. Since, these observations provide some experimental insight into the solvent contributions to the CT spectra, we have considered them in detail.

The shift in opposite directions of the (Ru^{II}/Ru^{III}) MM'CT and the (Ru^{II}(bpy)₂/bpy) MLCT spectra of (bpy)₂(CN)Ru(CNRu(NH₃)₅)³⁺ when the solvent is varied is a very striking observation, and it is consistent with a simple perturbational treatment of the solvent effects. The variations of $h\nu_{\max}$ with change of solvent for the MM'CT absorption of the bisruthenate are 35% greater than those of the monoruthenate, but there is an excellent correlation between the solvent shifts for the two complexes (Figure 4s⁶⁵). We also find that the shifts for both complexes correlate strongly with the respective variations in $\Delta E_{1/2}$ ($\Delta E_{1/2} = E_{1/2}[\text{Fe}(\text{Cp})_2^{+0}] - E_{1/2}[\text{Ru}(\text{NH}_3)_5^{3+,2+}]$) with $h\nu_{\max}$ increasing as $\Delta E_{1/2}$ increases (i.e., as Ru(NH₃)₅³⁺ is more stabilized by solvation), but the data are scattered (correlation coefficients ~ 0.9). There is a 160–210 meV difference in $h\nu_{\max}$ for the bis- and monoruthenates in all solvents examined, while $\Delta E_{1/2}$ for either varies only over the range of 0–70 mV. The largest part of this difference in $h\nu_{\max}$ for bis- and monoruthenates in any specific solvent probably arises from the contribution of $E_{1/2}(\text{Ru}(\text{bpy})_2^{3+,2+})$ to $\Delta E_{\text{ge}}^{\circ}$ since the difference between measured half-wave potentials of the (bpy)₂Ru(CNRu(NH₃)₅)(CNRh(NH₃)₅)^{7+,6+} and (bpy)₂(CN)Ru(CNRu(NH₃)₅)^{4+,3+} couples (in acetonitrile) also falls within this range. That this is the case is illustrated by the observation that the difference, $\Delta h\nu_{\max} = h\nu_{\max}(\text{MLCT}) - h\nu_{\max}(\text{MM'CT})$, for the Ru_c(II) → bpy and Ru_c(II) → Ru_t(III) absorptions, respectively, is correlated with $\Delta E_{1/2}(\text{Ru}(\text{NH}_3)_5^{3+,4+})$ (Figure 5s⁶⁵). That the differences between the energies of the absorption maxima of the Ru^{II}(bpy)₂ → Ru^{III}(bpy^{*})(bpy)^{*} and the (bpy)₂Ru^{II}(CNRu^{III}(NH₃)₅) → (bpy)Ru^{III}(CNRu^{II}(NH₃)₅) CT transitions are so simply correlated with $\Delta E_{1/2}(\text{Ru}(\text{NH}_3)_5^{3+,2+})$ indicates that (a) these contributions to the absorption energies can be treated as a simple linear combination of the contributions of the electron transfer components and (b) the solvational interactions are largely dominated by interactions of the Ru(NH₃)₅^{3+,2+} couple. The latter point is consistent with Richardson's analysis of the solvent dependence of the Ru(bpy)₃^{3+,2+} and Ru(NH₃)₆^{3+,2+} redox couples.⁷⁵ That $h\nu_{\max}(\text{MLCT})$ and $h\nu_{\max}(\text{MM'CT})$ vary in nearly opposite senses as the solvent is varied suggests that solvation of the Ru(bpy)₂^{3+,2+} couple cannot be neglected; a simple way of rationalizing these trends in CT absorptions is

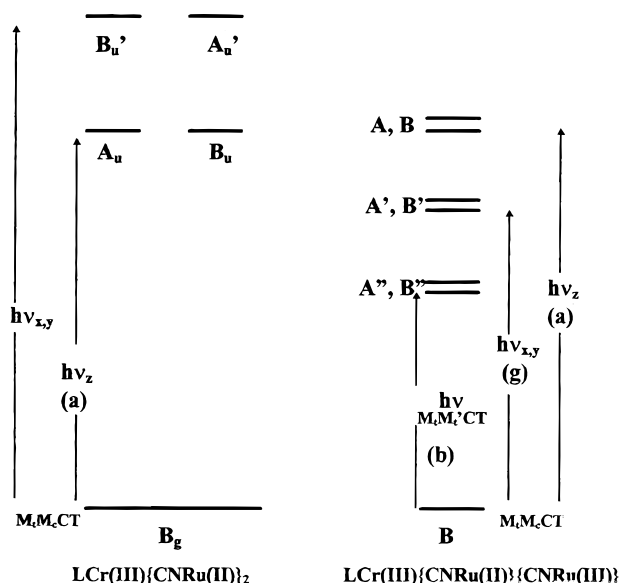


Figure 5. Comparison of MM'CT transitions expected for LM(CNRu^{II})₂ (left side) and LM(CNRu^{II})(CNRu^{III}) (right side) complexes. The symmetries assumed in this illustration are for (*trans*-[14]aneN₄)-Cr(III)-centered complexes. The higher energy $h\nu_{xy}$, components of the LM(CNRu^{II})₂ complexes have not been identified. All three components appear in the LM(CNRu^{II})(CNRu^{III}) spectra (where M is a $d\pi$ donor or a $d\pi$ acceptor). The dominant absorption in each case is assigned as $h\nu_z$. Subscripts: c, central metal; t, terminal metal.

to attribute most of the solvation effect to the solvation of the Ru(III) centers and that this effect is about twice as large for Ru(NH₃)₅³⁺ as for Ru(bpy)₂³⁺ (this is based on the 2-fold ratio of external radii and the inverse dependence of solvation energy on this parameter; this is reasonably consistent with the opposite trends of MLCT and MM'CT spectra considered here). These points may be compactly summarized in terms of eqs 2⁷⁶–5⁷⁷

$$h\nu_{\max}(\text{DACT}) \cong E_{\text{eg}}^{\circ} + \lambda \quad (2)$$

$$FE_{1/2}(\text{A/A}) \cong FE_{1/2}^{\circ}(\text{A/A}^{-}) - \epsilon_s \quad (3)$$

$$FE_{1/2}(\text{D/D}^{-}) \cong FE_{1/2}^{\circ}(\text{D/D}^{-}) + \epsilon_s \quad (4)$$

$$E_{\text{eg}}^{\circ} \cong FE_{1/2}^{\circ}(\text{D/A}) + 2\epsilon_s + T\Delta S \quad (5)$$

for a D/A complex in which DACT mixing stabilizes the ground state by an amount of ϵ_s , the superscript ^o refers to the redox couples in the absence of D/A mixing, F is the Faraday constant, and we will generally ignore the entropy contributions ($T\Delta S$). The solvent will generally contribute to both $\Delta E_{1/2}^{\circ}(\text{D/A})$ and to λ . If we represent the relative variations in these contributions with respect to some reference ("ref") medium as $\delta_m(\text{X})$ and $\gamma_m(\text{Y})$ for the complex fragments X (Ru(NH₃)₅, Ru(bpy), bpy) and for the electron-transfer couples Y, respectively, and if we assume that contributions to these variations are linearly additive,⁷⁹ then the solvent (or medium, m) dependence can be described using terms in the curly brackets of eqs 6 and 7, where

$$h\nu_{\max}(\text{DACT}) \cong F\Delta E_{1/2}^{\text{ref}}(\text{D/A}) + \lambda^{\text{ref}} + \{\delta_m(\text{D}) - \delta_m(\text{D}^{-}) - \delta_m(\text{A}) + \delta_m(\text{A}^{-}) - \gamma_m(\text{D/D}^{-}) + \gamma_m(\text{A/A}^{-})\} \quad (6)$$

$$F\Delta E_{1/2}(\text{D/A}) \cong F\Delta E_{1/2}^{\text{ref}}(\text{D/A}) + \{\delta_m(\text{D}) - \delta_m(\text{D}^{-}) - \delta_m(\text{A}) + \delta_m(\text{A}^{-})\} \quad (7)$$

we have introduced the abbreviations $\text{A/A}^{-} = \text{Ru}(\text{NH}_3)_5^{3+,2+}$ and $\text{D/D}^{-} = \text{Ru}(\text{bpy})_2^{3+,2+}$. Then our observations, comple-

mented by charge density considerations, on the complexes suggest that the relative solvent perturbations are ordered as $(\text{B/B}^{-} = \text{bpy}^{0,-})$: (a) $|\delta_m(\text{A})| > |\delta_m(\text{D})| > |\delta_m(\text{A}^{-})| > |\delta_m(\text{D}^{-})| > |\delta_m(\text{B}^{-})| > |\delta_m(\text{B})|$; and (b) $|\gamma_m(\text{A/A}^{-})| > |\gamma_m(\text{D/D}^{-})| > |\gamma_m(\text{B/B}^{-})|$. The MLCT absorption maximum can now be represented as in eq 8. Then the difference $\Delta h\nu = h\nu_{\max}$

$$h\nu_{\max}(\text{MLCT}) \cong F\Delta E_{1/2}^{\text{refb}}(\text{D/B}) + \lambda_{\text{DB}}^{\text{refb}} + \{\delta_m(\text{D}) - \delta_m(\text{D}^{-}) - \delta_m(\text{B}) + \delta_m(\text{B}^{-}) + \gamma_m(\text{B/B}^{-}) - \gamma_m(\text{D/D}^{-})\} \quad (8)$$

(MLCT) - $h\nu_{\max}(\text{DACT})$ is given by eq 9, where Δ_{ab} is the

$$\Delta h\nu \cong \Delta_{\text{ab}} + \{\delta_m(\text{A}) - \delta_m(\text{A}^{-}) - \delta_m(\text{B}) + \delta_m(\text{B}^{-}) + \gamma_m(\text{B/B}^{-}) - \gamma_m(\text{A/A}^{-})\} \quad (9)$$

collection of solvent(m) independent terms from eqs 6 and 8. The observations on these complexes and the inferences noted above suggest that terms involving the pentaamine moieties are dominant and that the simpler form of eq 10 is sufficient. The

$$\Delta h\nu \cong \Delta_{\text{ab}} + \{\delta_m(\text{A}) + \gamma_m(\text{B/B}^{-}) - \gamma_m(\text{A/A}^{-})\} \quad (10)$$

experimental half-wave potentials can be represented as in eq 11, with $\text{C}^+/\text{C} = \text{Fe}(\text{Cp})_2^{+,0}$. A comparison of eqs 10 and 11

$$F\Delta E_{1/2}^{\text{obsd}} \cong F\Delta E_{1/2}^{\text{refc}}(\text{C/A}) + \{\delta_m(\text{C}^+) - \delta_m(\text{A}) - \delta_m(\text{C}) + \delta_m(\text{A}^{-})\} \quad (11)$$

to Figure 4s suggests eq 12. Approximations based on the

$$\{\delta_m(\text{A}) + \gamma_m(\text{B}^+/\text{B}^{-}) - \gamma_m(\text{A/A}^{-})\} \approx -2\{\delta_m(\text{C}^+) - \delta_m(\text{A}) - \delta_m(\text{C}) + \delta_m(\text{A}^{-})\} \quad (12)$$

relative sizes of the solvent perturbations, discussed above lead to the conclusion that in $(\text{bpy})_2\text{Ru}(\text{CNRu}(\text{NH}_3)_5)_2^{6+}$ the effect of solvent variations on the half-wave potential of the Ru-(NH₃)₅^{3+,2+} couple are approximately compensated by the concomitant changes in solvent reorganizational energy, eq 13.

$$\gamma_m(\text{A/A}^{-}) \approx -\delta_m(\text{A}^{-}) \quad (13)$$

This near equality of $\gamma_m(\text{A/A}^{-})$ and $-\delta_m(\text{A})$, inferred from Figure 5s, is not so obvious, but it is not unreasonable.

Overall, our observations on the solvent dependent properties of the $(\text{bpy})_2(\text{CN})_{2-n}\text{Ru}(\text{CNRu}(\text{NH}_3)_5)_n^{3m+}$ complexes shows that these are dominated by the solvent dependence of the Ru-(NH₃)₅³⁺ moiety and that the Ru(bpy)₂³⁺ center plays a much smaller, but sometimes important, role. An extension of eq 13 which is useful in arguments employed in the Discussion section is that the contributions of solvation energies to $E_{1/2}(\text{Ru}(\text{NH}_3)_5^{3+,2+})$ can be approximated by the solvational contribution to λ_r .

5. Some Observations on the Mixing of CT Excited States in the CN⁻-Bridged Complexes. Some points have already been noted above. The most dramatic manifestations of the mixing between chromophores in these systems is illustrated by the $(\text{bpy})_2\text{Fe}(\text{CNRu}(\text{NH}_3)_5)_2^{6+,4+}$ redox titrations (Figure 3; we observe very similar behavior for the phen analogue). If this is compared to Figure 2, it is evident that the dominant Fe(II) → bpy MLCT absorption, which occurs at 520 nm in Fe(bpy)₂(CN)₂ and which would most likely be assigned at 545 nm in the reduced complex or 470 nm in the oxidized complex, shifts dramatically upon oxidation of the terminal Ru(NH₃)₅²⁺ moiety, while a much smaller (~10 nm) shift of the analogous

absorption is observed in the Ru(II)-centered complex. It is further evident that the Fe(II) \rightarrow bpy MLCT absorption occurs very near the energy of the Ru(NH₃)₅²⁺ \rightarrow bpy absorption in the other, related complexes (20.6×10^3 and 21.6×10^3 cm⁻¹, respectively, for the Ru(II)(bpy)₂ and Cr(III)(bpy)₂ analogues; Table 2). This behavior of the Fe(II)(PP)₂ complexes is strong evidence for significant mixing between the central metal M_c \rightarrow PP MLCT (M_c = Fe(II) or Ru(II)) and the "remote" Ru(NH₃)₅²⁺ \rightarrow PP MLCT excited states.^{77,78} The effects of this proposed mixing are illustrated in the inset of Figure 3.

While the intensities of the deconvoluted Ru(NH₃)₅²⁺ \rightarrow bpy transitions have to be regarded as relatively uncertain, especially in the Ru(II) complex, there is a general trend for these absorptions to be most intense when there is a neighboring CT absorbance (Table 2). This apparent "intensity stealing" is further, qualitative support for mixing of the CT states.²

While the evidence is strongest for mixing of the M \rightarrow bpy MLCT excited states, because they are so similar in energy, there is more limited spectroscopic evidence for mixing of most of the CT states of these complexes. Evaluation of such interactions is very difficult for the higher energy CT excited states owing to their large number and to the convolution of their overlapping absorptions in most of the complexes.

Mixing of the MM'CT excited states with Ru(NH₃)₅²⁺ \rightarrow CN⁻(π^*) or with the CN⁻(π) \rightarrow Ru(NH₃)₅³⁺ LMCT excited states is also symmetry allowed. The CT spectra of (H₃N)Rh-(CNRu(NH₃)₅)⁴⁺ are consistent with significant mixing of these chromophores, analogous to the effects observed in the Fe(II) polypyridyl complexes. It is generally difficult to identify clear spectroscopic evidence of such mixing largely because we cannot properly account for the effects of the many high-energy transitions that are possible and observed and in some instances because there is ambiguity in assigning the transitions.

Overall, the CN⁻/Ru MLCT and LMCT absorption spectra and the Ru_i/bpy MLCT spectra are consistent with the mixing of these states with the MM'CT excited states of concern in this paper.⁸⁰ The effects are relatively small for some of these states, as expected on the basis of their energy differences. The spectroscopy of these complexes does indicate that any symmetry-allowed mixing of CT states must be taken into account in dealing with these systems.⁸¹ The further implications of this will be developed below.

B. The Patterns of Variation in $E_{1/2}$ for the LM(CNRu(NH₃)₅)^{3+/2+} Couples. The redox potential of the Ru(NH₃)₅^{3+/2+} couple in these complexes was found to span a range of 350 mV in acetonitrile (see Tables 2 and 1s). It tends to the more positive values for species in which the Ru(II) form is stabilized by mixing of the ground state with the MM'CT excited state and to more negative values when this mixing stabilizes the Ru(III) form. Only one voltammetric wave was observed for the bismetalates, with a peak-to-peak distance about 20% larger than for the respective monometalates. The value of $E_{1/2}$ for the Ru(NH₃)₅^{3+/2+} couple of the (bpy)₂Ru(CNRu(NH₃)₅)₂(LAS)₆ complex in acetonitrile was found to be 0.022 ± 0.010 V (referenced to Fe(Cp)₂⁺⁰ with excess LAS).

There is a rough correlation of the variations in $E_{1/2}$ (Ru(NH₃)₅^{3+/2+}) with the oscillator strength of the MMCT absorption band (Figure 6), but the "slopes" and "intercepts" differ for series of complexes with different nonbridging ligands. The apparent "slopes" vary over a 4-fold range, with the most shallow found for the (MCL)M(CNRu(NH₃)₅)₂⁵⁺ complexes and the steepest for the (bpy)₂(CN)M(CNRu(NH₃)₅)ⁿ⁺ complexes. There are a number of complications in evaluating these apparent slopes: (a) ϵ_s^{op} is probably greater than zero for the Rh(III)-centered "reference" compounds, as mentioned above;

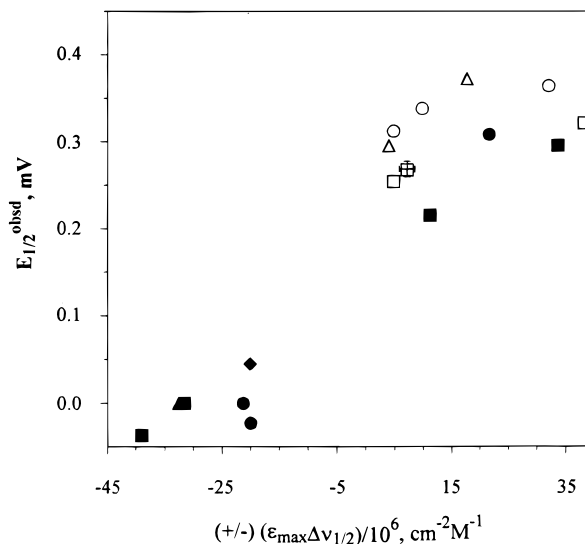


Figure 6. Graphical representation of the variations in $E_{1/2}^{\text{obsd}}$ with the oscillator strength of the MM'CT absorption band for some (L)M-(CNRu(NH₃)₅)ⁿ⁺ complexes: L = (bpy)₂, $n = 2$; ●, L = (bpy)₂, $n = 1$; ▲, M = Fe(II), L = (phen)₂, $n = 2$; ◆, L = (tpy)(bpy), $n = 1$; +, (bpy)₂Ru(CNRh(NH₃)₅(CNRu(NH₃)₅)⁶⁺); □, L = *ms*-Me₆[14]aneN₄, $n = 2$; ○, L = [14]aneN₄, $n = 2$; △, L = (NH₃)₅, $n = 1$; +, L = [15]-aneN₄, $n = 2$. The "−" sign is chosen for Ru(NH₃)₅³⁺ adducts, the "+" sign for Ru(NH₃)₅²⁺ adducts.

(b) the symmetry constraints for optical absorption are different from those for the mixing of excited and ground states in these different series of complexes;⁸⁰ (c) there is a change of charge type for the complexes at the extremes of the polypyridyl series, and this may lead to different solvational contributions; (d) changes in the nonbridging ligand result in changes of $E_{1/2}$ which are also likely to be solvational in origin. Each of these points will be addressed in the discussion below.

The M(bpy)₂^{3+/2+} couples were nearly reversible for M = Ru and Fe and quasireversible for M = Cr. We also found the Co(III)–(II) couple of *trans*-Co([14]aneN₄)(CN)₂⁺ (in DMSO) and *trans*-Co([14]aneN₄)(CNRu(NH₃)₅)₂⁵⁺ (in acetonitrile) to be quasireversible ($E_{1/2}(\Delta E_p) = -1.279 \pm 0.005$ (96) and -1.254 ± 0.006 (160), respectively, vs SCE and referenced to Fe(Cp)₂⁺⁰). Observations on the parent complexes are summarized in Table 2s.

A few Ru(NH₃)₅⁵⁺ half-wave potentials were determined in water using a glassy carbon electrode. The $E_{1/2}$ values in water were more negative than those in acetonitrile by an average of 93 (± 22) mV, independent of charge type (all referenced to Fe(Cp)₂⁺⁰).

C. Some Symmetry Considerations. We have noted above that symmetry considerations play an important role in evaluating our observations on the trimetallic complexes. The symmetry-adapted metal-centered ($d\pi$ or $d\sigma$) orbitals for pertinent complex geometries, maximum symmetry of C_{2v} for cis and C_{2h} for trans (note that the C₂ axes pass through only the central atom in either case), and the resulting MM'CT excited-state symmetries are presented in Table 5. For the terminal Ru(NH₃)₅ moieties we have only considered the $d\pi$ orbitals (i.e., the two orbitals parallel to the MM' axis), but for the central metals we have taken into account all the lowest energy acceptor orbitals.

The (bpy)₂Ru(CNRu(NH₃)₅)₂⁶⁺ complex is the most complicated of those that we have considered, largely due to the nominal degeneracy of the two $d\pi$ holes at the terminal Ru(NH₃)₅³⁺ moieties. Thus, there are six different potential ground-state electronic configurations of this complex, which differ only in the arrangement of the holes in the symmetry-adapted Ru(II) \rightarrow $d\pi$ orbitals. If all these configurations are

TABLE 5: Orbital and Electronic-State Symmetries for LM_c(CNRu_t(NH₃)₅)₂ Complexes

maximum molecular symmetry	central metal ^a	ground state ^{a,b}		excited state		
		electronic configurations	symmetry	electron configurations ^c	symmetry ^d	
<i>C</i> _{2v}	Ru ^{III} _c (<i>t</i> _{2g} : a ₁ , a ₂ [′] , b ₁ [′])	or	(a ₁ , b ₂) _t	B ₂	(a/a ₂ [′] /b ₁ [′]) _c (a ₁ /b ₂) _t	A ₁ , B ₂ , A ₂ , (B ₁), (B ₁), A ₂
		or	(a ₁ , a ₂) _t	A ₂	(a ₁ /a ₂ [′] /b ₁ [′]) _c (a ₁ /a ₂) _t	(A ₁), A ₂ , A ₂ , (A ₁), B ₁ , B ₂
		or	(a ₁ , b ₁) _t	B ₁	(a ₁ /a ₂ [′] /b ₁ [′]) _c (a ₁ /b ₁) _t	A ₁ , B ₁ , A ₂ , (B ₂), B ₁ , A ₁
		or	(a ₂ [′] , b ₁ [′]) _t	B ₂	(a ₁ /a ₂ [′] /b ₁ [′]) _c (a ₂ [′] /b ₁ [′]) _t	A ₂ , (B ₁), A ₁ , B ₂ , B ₂ , A ₁
		or	(a ₂ [′] , b ₂) _t	B ₁	(a ₁ /a ₂ [′] /b ₁ [′]) _c (a ₂ [′] /b ₂) _t	A ₂ , (B ₂), A ₁ , B ₁ , (B ₂), A ₂
<i>C</i> _{2v}	Cr ^{III} _c (<i>t</i> _{2g} : a ₁ , a ₂ [′] , b ₁ [′])	or	(b ₁ [′] , b ₂) _t	A ₂	(a ₁ /a ₂ [′] /b ₁ [′]) _c (b ₁ [′] /b ₂) _t	B ₁ , B ₂ , B ₂ , B ₁ , (A ₁), A ₂
			(a ₁ , a ₂ [′] , b ₁ [′]) _c	B ₂	(a ₁ , a ₂ [′]) _c (a ₁ /b ₂ /a ₂ [′] /b ₁ [′]) _t	A ₂ , (B ₂), A ₁ , B ₂
<i>C</i> _{2v}	Rh(III)/Co(III) (e _g : a ₁ , b ₂)			A ₁	(a ₁ , b ₁ [′]) _c (a ₁ /b ₂ /a ₁ [′] /b ₁ [′]) _t	(B ₁), A ₂ , B ₂ , A ₁
				A ₁	(a ₂ [′] , b ₁ [′]) _c (a ₁ /b ₂ /a ₂ [′] /b ₁ [′]) _t	(B ₂), A ₁ , (B ₁), A ₂
<i>C</i> _{2h}	Cr(III) (<i>t</i> _{2g} : a _g , a _g [′] , b _g [′])		(a _g , a _g [′] , b _g [′]) _c	B _g	(a _g , a _g [′]) _c (a _g /b _g [′] /b _u /a _u [′]) _t	(A _g), B _g , B _u , A _u
				B _g	(a _g , b _g [′]) _c (a _g /b _g [′] /a _u /b _u /a _u [′]) _t	B _g , (A _g), A _u , B _u
<i>C</i> _{2h}	Rh(III)/Co(III) (e _g : a _g , b _g)			A _g	(a _g , b _g [′]) _c (a _g /b _g [′] /a _u /b _u /a _u [′]) _t	B _g , (A _g), A _u , B _u
				A _g	(a _g) _c (a _g /b _g /b _u /a _u [′]) _t	A _g , (B _g), B _u , A _u
				A _g	(b _g) _c (a _g /b _g /b _u [′] /a _u [′]) _t	(B _g), A _g , A _u , B _u

^a Subscripts: “t” = terminal; “c” = central. Metal-centered orbitals considered are designated *d* π for orbitals parallel (or at 45°) to the Ru–CN–Ru axis; *t*_{2g} and e_g refer to d orbitals so designated in *O*_h symmetry. The symmetry-adapted *d* π orbitals of two terminal Ru moieties are (a₁, b₂, a₂[′], b₁[′]) in *C*_{2v} and (a_g, b_u, a_u, b_g) in *C*_{2h}. ^b In *C*_{2v} symmetry the apostrophe refers to orbitals not in the Ru_c(Ru_t)₂ plane; in *C*_{2h} symmetry the apostrophe refers to orbitals not in the symmetry plane (σ_h). Note that the *C*₂ axis in *C*_{2h} is orthogonal to the Ru_c(Ru_t)₂ axis and bisects an equatorial N–Ru–N angle. ^c The slash (“/”) to be read as “or”. ^d Symmetries disallowed for electronic (dipole) absorptions and for mixing with the ground state are in parentheses. Excited states with proper symmetry to mix with the ground state are in italics.

similar in energy, then on the average only one excited-state configuration would mix with the ground state for every three allowed transitions if *C*_{2v} symmetry were applicable and all MM’CT components were equally weighted in each case. In *C*₂ symmetry the ratio would average 1/2. The same symmetry restrictions apply to the cis-complexes with Cr(III), Co(III), and Rh(III) centers.

The highest symmetry of the trans-complexes used in this study is *C*_{2h}, but lowering the molecular symmetry to approximately *C*₂ (with the [15]aneN₄ complexes) has no significant effect on the observations. This suggests that only the axial symmetry is important for D/A coupling-related issues. In view of this, and the fact that our cis-complexes all have maximum *C*₂ molecular symmetry, we have used the less restrictive *C*₂ symmetry in treating the observations.

This analysis assumes that all components of the dipole operator have equal weights for their contributions to the absorption intensity or in their mixing with the ground-state wave function.^{79,80}

Discussion

We began this study in order to obtain independent experimental measures of the electronic coupling parameters which appear to be important in determining the ~10⁴-fold range of back-electron-transfer rates in CN⁻-bridged D/A complexes.^{39,82–85} This had led us to compare the spectroscopic and electrochemical properties for several issues of CN⁻-bridged D/A complexes. A number of ground-state properties of the CN⁻-bridged D/A complexes have differed from our expectation when we began to study these systems several years ago.⁸⁶ Among the most striking examples are the unusual⁸⁷ shift to lower energies of ν_{CN} when the CN⁻ bridges a D/A pair, the proportionality of this shift to H_{DA}^2/E_{DA} , and the symmetry constraints on which CN⁻ modes (symmetric or antisymmetric) couple with H_{DA} .^{39,40,62} Such observations indicate that bridging ligands’ nuclear coordinates are coupled to H_{DA} . As a consequence we have examined ways in which the interaction between bridging ligand and donor–acceptor may alter the net behavior of the electron-transfer ground and excited states. An important aspect of this

issue has been the extent to which variations in the ground-state stabilization energy, which arises from D/A coupling, may be manifested in variations in the half-wave potential of the simple –Ru(NH₃)₅^{3+·2+} probe redox couple. Unfortunately, neither the variations of $E_{1/2}$ with H_{DA} nor the independent evaluation of H_{DA} has been a simple matter. Thus, the systematic variation of H_{DA} in a “homologous” series of compounds requires variations of some molecular functional groups, such as the nonbridging ligands or the donor or the acceptor, and such variations in the molecules inevitably cause variations in some other parameters, which also change the parameters measured, e.g., the solvational free energy, (ΔG_s). As a consequence, it has been necessary to examine several aspects of solvational effects and CT state mixing in several series of compounds before we have been able to extract information about how bridging ligand mediated D/A coupling might affect ground-state thermodynamic properties. The results are more or less consistent with those of Curtis and co-workers on very different substrates,⁴⁴ and they can be accounted for in terms of a pseudo-Jahn–Teller-like vibronic model involving bridging ligand nuclear coordinates, such as has been suggested elsewhere.^{28,33,39c,d,40}

A. Aspects of the MM’CT Spectroscopy. The dominant MM’CT band in these complexes is nearly Gaussian (with respect to an energy scale) in ambient solutions and is probably a convolution of several configurationally different components. Mixing with MLCT or LMCT states of the nonbridging ligands does not appear to have a significant effect on the oscillator strength.

The bisruthenates of LM(CN)₂ complexes (M = a *d* π donor or acceptor) exhibit a weak, relatively low energy Ru/M MM’CT component when the ruthenium moieties differ in oxidation state. This can be associated with an electronic transition that involves a central metal *d* π orbital which is not involved in coplanar *d* π (D)/*d* π (A) coupling. In a multicenter quasibonding model of the D/A coupling, the two components of the Ru/M MM’CT absorption in these “mixed valence” (Ru(III)/Ru(II)) complexes correspond to an *x*,*y*-allowed *d* π (D_{BMO}) → *d* π (A_{NBMO}) absorption at the lower energy and a *z*-allowed *d* π (D_{BMO}) → *d* π -

(A_{ABMO}) absorption at higher energy (where BMO corresponds to the multicenter D/A coupled ground-state orbital(s), ABMO corresponds to the corresponding excited-state “antibonding” orbital set, and NBMO is an acceptor orbital not involved in the coupling); see Figure 5.

B. Comparison of H_{DA} Dependent Ground-State Observables: MM'CT Absorption Intensity and $E_{1/2}^{\text{obsd}}$. Figure 6 strongly suggests a relationship between these observables, but it also suggests that evaluating it is bound to be complicated. To proceed, we must first consider what one might expect and then evaluate those factors that might complicate the comparison. The major complicating factors that we consider are the effects of electronic delocalization and of variations in solvation energies.

1. *Perturbational Models for the Relationship between the Variation of Ground-State Stabilization Energy, ϵ_s^{th} , and H_{DA} .* The variations in ϵ_s^{th} that result from D/A electronic coupling must be defined with respect to some uncoupled reference state, a diabatic state with respect to D/A coupling. For the systems discussed here, it would be useful to define reference states in terms of the properties of uncoupled, monometal complexes. In practice, no monometal complexes that are rigorously appropriate reference systems are available: such complexes typically differ in their coordination spheres, charge types, and/or solvational interactions. Alternatively, one might seek a substitution inert “reference” metal to substitute for D or A in di- and trimetallic complexes. Ideally, this reference metal should exhibit no D/A coupling, but this is equivalent to the unrealistic requirement that the cationic metal center used have no electron affinity (or ionization energy). Thus, the actual “experimental” reference parameters, such as $E_{1/2}^{\text{ref}}$, must always involve some sort of approximation or extrapolation. We have elected to use Rh(III)-centered complexes as approximate experimental reference compounds since the π/σ nature of the D/A coupling should lead to relatively small values of H_{DA} and since E_{DA} should be relatively large, so that one expects $\epsilon_s^{\text{th}} = H_{\text{DA}}^2/E_{\text{DA}}$ to be relatively small for such complexes. We have taken into account the major factors that might contribute to any differences between the values of parameters measured for the Rh(III)-centered reference compounds and an idealized reference complex. The simplest and most traditional, “Mulliken–Hush” level of treatment of D/A complexes, the evaluation of the relevant parameters based on the experimental measurements, and the comparison of the experimental observations to pertinent models are considered in this section.

2. *Contributions to H_{DA} .* In the simplest two-state limit any contributions of the bridging ligand are ignored or are assumed to be the same in the monometal components such as in the bridged D/A complex. Thus, one begins with knowledge of the unmixed, or diabatic limit (designated with a superscript \circ), so that the perturbationally corrected ground (subscript g) and excited (subscript e) state wave functions are given as in eq 14^{2–4} where $\Delta E_{\text{ge}}^{\circ}$ is the energy difference between the two

$$\psi_{\text{g}} = [\psi_{\text{g}}^{\circ} + (\beta_{\text{ge}}/\Delta E_{\text{ge}}^{\circ})\psi_{\text{e}}^{\circ}]N \quad (14\text{a})$$

$$\psi_{\text{e}} = [\psi_{\text{e}}^{\circ} - (\beta_{\text{ge}}/\Delta E_{\text{ge}}^{\circ})\psi_{\text{g}}^{\circ}]N \quad (14\text{b})$$

diabatic states (g and e), $\beta_{\text{ge}} = \langle \psi_{\text{g}}^{\circ} | H' | \psi_{\text{e}}^{\circ} \rangle - S_{\text{ge}} E_{\text{g}}^{\circ}$, the ψ_i° are wave functions of these states, H' is the perturbation Hamiltonian which allows their mixing, S_{ge} is an overlap integral, E_{g}° is the energy of the unperturbed ground state, and N is a normalization constant. Parameters measured in real systems must be defined in terms of “correct” wave functions, ψ_{g}' and ψ_{e}' , and the corresponding matrix elements can be expressed as $H_{\text{DA}} =$

$\langle \psi_{\text{g}}' | H' | \psi_{\text{e}}' \rangle$.⁴ In the simplest limit eqs 14 can be considered good approximations to the ψ_i' . In this limit, electronic coupling is in effect a very weak “bonding” interaction between D and A and may be referred to as “direct” coupling (H_{DA}^{d}).

The simplest way to allow for the contributions of a bridging ligand to H_{DA} is to add terms to eqs 14 that allow for the perturbational mixing of bridging ligand excited states with the electron-transfer ground and excited states. The important bridging ligand excited states in this context are the metal (D[−] or A[−]) to bridging ligand charge transfer (MLCT) and bridging ligand to metal charge transfer (D or A) excited states. This leads to a superexchange contribution to H_{DA} ,^{4,30} which can be written as in eqs 15–17⁴ in which the $H_{i\text{CT}}$ ($i = \text{D or A}$) are

$$H_{\text{DA}}^{\text{s}}(\text{MLCT}) = H_{\text{DCT}} H_{\text{ACT}} / \Delta E_{\text{av}} \quad (15)$$

$$H_{\text{DA}}^{\text{s}}(\text{LMCT}) = H_{\text{DCT}}' H_{\text{ACT}}' / \Delta E_{\text{av}} \quad (16)$$

$$\Delta E_{\text{av}} = 2E_{\text{DCT}} E_{\text{ACT}} / (E_{\text{DCT}} + E_{\text{ACT}}) \quad (17)$$

the electronic matrix elements for the MLCT transitions (involving the same bridging ligand molecular orbital) of the electron-transfer ground (D) and excited (A) states,⁸⁸ and the $E_{i\text{CT}}$ are the respective vertical (with respect to the ground-state equilibrium nuclear coordinates) energy differences (analogous definitions can be made for the LMCT states). Equations 15 and 16 are second-order perturbational corrections to H_{DA}^{d} and are expected to be important only when $H_{\text{DA}}^{\text{d}} \approx 0$. Reimers and Hush have generalized this argument and point out that if the PE minima of one of the electron-transfer states and the perturbing state are comparable, then much more complicated behavior than that implied by eqs 15 and 16 can be expected.⁸⁹ In the systems considered here the perturbing CT excited states (of CN^-) are much higher in energy than the energies of the electron-transfer states near their PE minima (however, this will not generally be true far from these PE minima; see discussion below). The superexchange model as sketched here does not allow for any problems in evaluating H_{DA} that might result from the changes in nuclear coordinates that accompany charge delocalization onto (or from) the bridging ligand, and it is generally applied assuming that H_{ACT} or H_{ACT}' have values that are independent of the nuclear coordinates (however, see also comments below).

Several authors have discussed electronic coupling models in which H_{DA} is a function of one or more of the nuclear coordinates associated with the electron-transfer process,^{28,32–35,47} i.e., $H_{\text{DA}} = H_{\text{DA}}^{\circ} + bx$, where H_{DA}° is the coordinate independent electronic coupling (possibly a sum of H_{DA}^{d} and H_{DA}^{s} , above), b is a linear vibronic constant,^{90–92} and x is the appropriate nuclear coordinate. Several features of the CN^- -bridged D/A complexes, some mentioned above, some reported in this study, have led us to consider a simple vibronic model for D/A coupling in these systems.^{39–41} We have searched for a relatively simple vibronic model that would have the potential of encompassing all the observed features of these systems. A simple, semiclassical vibronic model seems able to do this^{39–41} (see Appendix B). This model involves a synergistic mixing of “local” (donor/bridging ligand and bridging ligand/acceptor) MLCT and LMCT excited states with the ground and MM'CT excited states, and this synergism is inferred to lead to an enhancement of the MLCT/LMCT mixing to stabilize the ground state. To display the qualitatively important features of the argument in an algebraically simple way, we have treated the MLCT and LMCT parameters (stabilization energies, reorganizational energies, coupling matrix elements, etc.) as the

“averaged” contribution of a single CT state. This leads to a ground (g) and MM’CT excited state (e) energies which are corrected for coupling to the higher energy CT state(s) as in eq 18,^{90–92} where E_{DA} is the energy difference between the ground

$$\begin{aligned} V_g &= kx^2 - ax \\ V_e &= E_{DA} + kx^2 + ax \end{aligned} \quad (18)$$

and MM’CT excited states before the vibronic perturbation, and it assumed that the force constants of the ground and excited states are equal (k). This argument leads to eq 19 for H_{DA}

$$H_{DA}^v \cong H_{DA}^o + \alpha_{CT}(\lambda_{CT}\lambda_{DA})^{1/2} + \alpha_{DA}\lambda_{DA} \quad (19)$$

evaluated at the ground-state equilibrium nuclear coordinates, where the α_i ($i = CT$ or DA) are the coefficients (H_{D_i}/E_{D_i}) for mixing the respective diabatic state functions with the ground state (the α_i^2 are the respective fractions of charge delocalized) and the λ_i are the correlated nuclear reorganizational energies. The perturbational corrections given by eq 19 are superficially similar to those given by eqs 15 and 16 in that they can be viewed as products of an effective mixing coefficient and an energy; however, they are qualitatively different in that the additional terms in eq 19 allow for the changes of H_{DA} with the horizontal displacement of the ground-state PE minimum and in that the perturbational changes are weighted by a nuclear reorganizational energy rather than by an electronic matrix element.

3. *The Expected Relationships between $E_{1/2}^{obsd}$, the Ground-State Stabilization Energy, ϵ_s^{th} , and H_{DA} .* In the simple two-state model sketched above, the mixing described by eqs 14 leads to stabilization of the ground state by an amount given by eq 20 if $E_{DA} \gg 2|H_{DA}|$.^{2,4} When the donor and acceptor are

$$\epsilon_s = H_{DA}^2/E_{DA} \quad (20)$$

redox labile transition metal complexes, oxidation of the donor center (or reduction of the acceptor) will remove that center from the CT coupling. Consequently, the electrochemical half-wave potentials are expected to vary systematically with ϵ_s as in eq 21,^{39,40} where $E_{1/2}^{ref}$ is the half-wave potential (e.g., for the

$$E_{1/2}^{obsd} = E_{1/2}^{ref} \pm \epsilon_s^{th} \quad (21)$$

A/A⁻ couple of a D/A pair) when there is no CT coupling and the sign of ϵ_s is determined by which component of the particular couple (e.g., A or A⁻) is stabilized by the CT coupling. In the limit that D/A coupling is dominated by “transfer” (or local dipole) terms (i.e., if there is significant direct overlap of the donor and acceptor orbitals of the ground state),² a simple model for the transition dipole in an electronic absorption can be used to give the electronic matrix element as in eq 22, where r_{ge}^c is

$$H_{DA}^{op} \cong \frac{0.0205}{r_{ge}^c} [\epsilon_{max} \Delta\nu_{1/2} \nu_{max}]^{1/2} \quad (22)$$

the distance (in Å) between the effective centers of charge of states e and g;^{2,4,7,29,48,51} $\nu_{max}\epsilon_{max}$ and $\Delta\nu_{1/2}$ are the frequency and molar absorptivity of the absorption maximum and the full width at half-maximum of the corresponding CT absorption band. If significant charge is delocalized in the various CT mixings, as discussed above, then r_{ge}^c should differ from the equilibrium distance between the geometrical centers of donor and acceptor, r_{DA} . Electroabsorption measurements have generally suggested that $r_{ge}^c < r_{DA}$.^{48,50,52} There are several factors

that seem to contribute to this inequality.^{29a,51} However, a major factor, and a sufficient factor for treating some of the trends of our observations, is the manner in which electronic charge is delocalized in the electron-transfer ground and excited states. This can be approximately treated with simple perturbation theory arguments, since the charge delocalized along the D/A axis, onto (or from) a bridging ligand, or between D and A, will have the effect of reducing the distance over which one unit of electronic charge (q_{el}) is transferred. Alternatively, the delocalization can be interpreted as reducing the charge difference (q_{eff}) between the D and A centers. If we assume that $q_{eff}r_{DA} \cong q_{el}r_{ge}^c$ ^{29a} and that charge transferred onto (or from) the bridging ligand is localized at its center, then $r_{ge}^c \approx r_{DA}(1 - 2\alpha_{DA}^2 - 3\alpha_{CT}^2/2)$ ⁹³ where α_{CT} is a sum over ground- and excited-state contributions. If there is additional delocalization onto the nonbridging ligands, L, then eq 23 may be more applicable,

$$r_{ge}^c \approx r_{DA}(1 - 2\alpha_{DA}^2 - (1.5\alpha_{CT}^2 - f\alpha_L^2)) \quad (23)$$

where f takes account of the spatial distribution of this last component of delocalized charge and the sum over ground- and excited-state contributions. Equation 23 is qualitatively useful to focus aspects of our discussion, but the actual weights of the perturbation terms represented are not clear and some ab initio calculations indicate that the most heavily weighted contributions occur for components which lie along the D–A axis.^{29b} Furthermore, although eq 23 has components that are conceptually reasonable, it suggests that there is limited physical basis for simple correlations of $E_{1/2}^{obsd}$ and ϵ_s^{op} and that for large DACT oscillator strengths (h_{DA}) each complex should be treated as a separate system.

For purposes of our discussion we will define an experimental parameter, $H_{DA}^{op'}$, which is based on the observed MM’CT absorption as in eq 24. We can then define an empirical

$$H_{DA}^{op'} = \frac{0.0205}{r_{DA}} [\epsilon_{max} \Delta\nu_{1/2} \nu_{max}]^{1/2} \quad (24)$$

parameter, ϵ_s^{op} , in which the only variables are the oscillator strength and the vertical energy difference, $E_{DA} = h\nu_{max}$,⁷⁶ as in eq 25.

$$\epsilon_s^{op} = (H_{DA}^{op'})^2/h\nu_{max} \quad (25)$$

4. *The Evaluation of ϵ_s^{op} from MM’CT Spectra.* The combination of eqs 24 and 25 yields eq 26, in which the constant

$$\epsilon_s^{op} \cong m(\epsilon_{max} \Delta\nu_{1/2}) \quad (26)$$

of proportionality $m = (0.0205/r_{DA})^2 = 1.55 \times 10^5$ cm for our CN⁻-bridged complexes. Equations 21 and 26 are the basis for the comparison in Figure 7. One possible interpretation of the apparently different values of m for the different series of complexes would be that r_{ge}^c differs in a systematic way from one series of complexes to another (see the preceding discussion). Before we can comment further on this, we must deal with some additional issues.

5. *The Evaluation of ϵ_s^{th} : Symmetry and Solvational Corrections.* a. *Symmetry Corrections.* The ground- and excited-state symmetries of the ground and MM’CT excited states for the cis-(C_{2v}) and trans-(C_{2h}) complexes are summarized in Table 5. We have used the less restrictive C₂ symmetry, which distinguishes only A and B representations, for the cis-LM-(CNRu(NH₃)₅)₂ complexes. Thus, for the cis- and trans-bisruthenates we have in effect correlated $E_{1/2}^{obsd}$ with ϵ_s^{op} per Ru

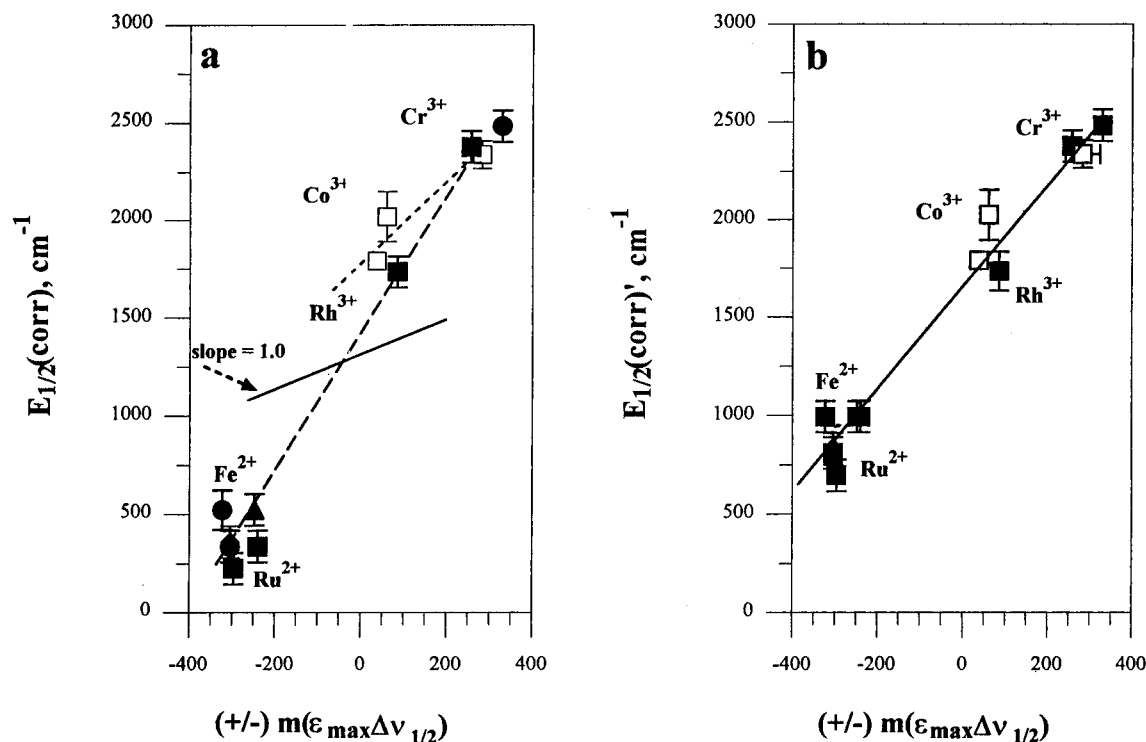


Figure 7. Correlation between $E_{1/2}^{\text{corr}}$ and oscillator strength per $\text{Ru}(\text{NH}_3)_5$ for some CN^- -bridged D/A complexes. $E_{1/2}^{\text{obsd}}$ from Figure 6 has been corrected for (a) differences in solvation originating from nonbridging ligands and (b) charge type $+950 \text{ cm}^{-1}$ for $\text{Ru}(\text{II})$ - and $\text{Fe}(\text{II})$ -centered dicyano complexes; this may include about 350 cm^{-1} contribution from excited-state LMCT coupling. See text for details. The data points are labeled as in Figure 6. The constant of proportionality is $m = 15.25 \times 10^{-6} \text{ cm}^{-1}$; values correspond to ϵ_s^{op} with $r_{\text{ge}}^c = r_{\text{DA}}$. Sign convention as in Figure 6.

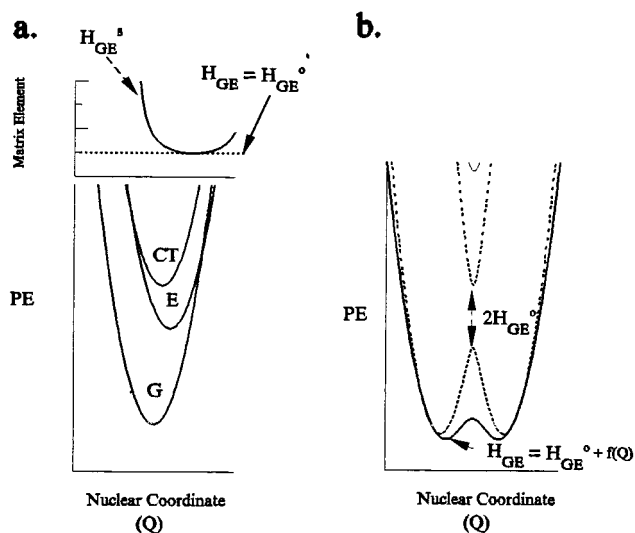


Figure 8. Qualitative illustration of the variations of H_{DA} with nuclear coordinates in a superexchange model (left) and the contrasting effects on the ground-state adiabatic potential energy surface of a reaction coordinate independent H_{DA} (Condon approximation and a vibronic type of coordinate dependence of H_{DA}) (right). The upper figure presumes that the D⁻A and DA⁻ diabatic PE surfaces are coupled through mixing with a higher energy CT surface as in the lower portion of the upper figure. A perturbational mixing of the two degenerate electron-transfer surfaces in the lower figure used electronic matrix elements $H_{\text{DA}} = H_{\text{DA}}^0 + f(Q)$. The function $f(Q)$ was chosen so that H_{DA} increased nearly linearly with Q when moving from either PE minimum toward the surface crossing, so that $H_{\text{DA}} = H_{\text{DA}}^0$ at the PE minima of the diabatic surfaces, and so that H_{DA} would increase for large displacements away from the surface crossing point (somewhat mimicking the superexchange behavior, top left).

in Figure 7, since in both C_2 and C_{2h} symmetry only one MMCT excited state (on the average) has the proper symmetry to mix with the ground state for every two states for which optical

absorption is allowed. This correction eliminates most of the discrepancy between the mono- and bisruthenates of the $\text{M}(\text{bpy})_2(\text{CN})_2^{n+}$ complexes.

b. The Effect of Charge Differences on $E_{1/2}^{\text{obsd}}$. The $(\text{bpy})_2(\text{CN})\text{M}(\text{CNRu}(\text{NH}_3)_5)^{3+,2+}$ ($\text{M} = \text{Ru}^{2+}$ or Fe^{2+}) couples differ by one charge unit from $(\text{L})(\text{CN})\text{M}(\text{CNRu}(\text{NH}_3)_5)^{4+,3+}$ ($\text{M} = \text{Rh}^{3+}$, Co^{3+} , or Cr^{3+}) couples. This difference could affect $E_{1/2}^{\text{obsd}}$ for the $\text{Ru}(\text{II})$ - and $\text{Fe}(\text{II})$ -centered polypyridyl complexes through either or both of the following: (i) differences in solvation energy (even though the charge difference nominally resides at the M center and our basic comparison is of the $\text{Ru}(\text{NH}_3)_5^{3+,2+}$ couples) or (ii) differences in the bridging $\text{CN}^-/\text{Ru}(\text{NH}_3)_5$ bonding (e.g., from electrostatic “induction” or an “internal Stark effect”). In general, $E_{1/2}^{\text{obsd}}$ tends to increase with increases in positive charge. This feature is illustrated in the differences in $E_{1/2}^{\text{obsd}}$ for four pairs of the D/A complexes discussed in this paper (Table 6). These experimental comparisons suggest that a one unit increase in charge increases $E_{1/2}^{\text{obsd}}$ by about $65 \pm 15 \text{ mV}$, and we have made the corresponding adjustment ($524 \pm 20 \text{ cm}^{-1}$) to $E_{1/2}^{\text{obsd}}$ for the $\text{Ru}(\text{II})$ - and $\text{Fe}(\text{II})$ -centered polypyridyl complexes in Figure 7a (i.e., for these complexes $E_{1/2}^{\text{corr}} \cong E_{1/2}^{\text{obsd}} + 524 \text{ cm}^{-1}$).

c. The Effects of Charge Delocalization on $E_{1/2}^{\text{obsd}}$. The electronic coupling of donor and acceptor leads to some fractional charge delocalization (α_{DA}^2). For the $\text{Cr}(\text{III})$ and $\text{Ru}(\text{III})$ complexes discussed here $\alpha_{\text{DA}}^2 \leq 0.1$, and, based on the comments in the preceding section, one would expect that this should contribute less than 10 mV to any measured value of $E_{1/2}$. Because solvation depends on charge density (see Results section A and Appendix A), there is an asymmetry in the effects of charge delocalization in these complexes (eq A11 of Appendix A) and this might affect our observations. Charge delocalization decreases $E_{1/2}^{\text{obsd}}$ in all the D/A complexes, and

TABLE 6: Effect of Complex Charge on $E_{1/2}^{\text{obsd}}$ ^a

complex ^b	couple ^b	overall charge type of couple	$E_{1/2}^{\text{corr}}$, V	$\Delta E_{1/2}$ mV ^d
(A) ₅ Cr(CNRu(A) ₅) ⁴⁺	Ru(A) ₅ ^{3+,2+}	5+/4+	0.372	49
([14]aneN ₄)(CN)Cr(CNRu(A) ₅) ³⁺	Ru(A) ₅ ^{3+,2+}	4+/3+	0.323 ^c	
(tpy)(bpy)Ru(CNRu(A) ₅) ⁴⁺	Ru(A) ₅ ^{3+,2+}	4+/3+	0.045	68
(bpy) ₂ (CN)Ru(CNRu(A) ₅) ³⁺	Ru(A) ₅ ^{3+,2+}	3+/2+	-0.023	
(bpy) ₂ Ru(CNRu(A) ₅)(CNRh(A) ₅) ⁶⁺	Ru(bpy) ₂ ^{3+,2+}	6+/5+	1.340	62
(bpy) ₂ (CN)Ru(CNRu(A) ₅) ³⁺	Ru(bpy) ₂ ^{3+,2+}	4+/3+	1.155	
(tpy)(bpy)Ru(CNRu(A) ₅) ⁴⁺	Ru(tpy)(bpy) ^{3+,2+}	5+/4+	1.235	80
(bpy) ₂ (CN)Ru(CNRu(A) ₅) ³⁺	Ru(bpy) ₂ ^{3+,2+}	4+/3+	1.155	
			ave	65 ± 13

^a Data from Tables 1 and 1s. ^b A = NH₃. ^c Corrected to identical ϵ_s^{op} using the empirical correlation (-5 mV for the ([14]aneN₄)(CN)-Cr(CNRuA₅)^{4+,3+} couple). ^d Apparent effect of one unit increase in charge.

TABLE 7: Relative Effects on $E_{1/2}(\text{Ru}(\text{NH}_3)_5^{3+,2+})$ of Changes in Nonbridging Ligands L in LM(CNRu(NH₃)₅)^{a,b}

L	M		
	Rh(III)	Co(III)	Cr(III)
(bpy) ₂	-40 ± 14		-24 ± 8
<i>t</i> -Me ₆ (14)aneN ₄	+58 ± 12	+72 ± 15	+43 ± 7
[15]aneN ₄		1 ± 10	
(NH ₃) ₅	31 ± 10		43 ± 9

^a $E_{1/2}(\text{Ru}(\text{NH}_3)_5^{3+,2+})$, for L(CN)_{2-n}M(CNRu(NH₃)₅)_n⁽¹⁻²ⁿ⁾⁺ minus $E_{1/2}(\text{Ru}(\text{NH}_3)_5^{3+,2+})$ for ([14]aneN₄(CN))_{2-n}M(CNRu(NH₃)₅)_n⁽¹⁺²ⁿ⁾⁺ (*n* = 1 or 2). Error limits represent the sum of standard deviations in $E_{1/2}^{\text{obsd}}$ measurements. Where data are available, values for mono- and bisruthenates have been averaged. ^b Average of relative solvent effects in mV due to nonbridging ligands: (bpy)₂, -30 ± 13; *trans*-Me₆[14]aneN₄, 54 ± 15; *trans*-[15]aneN₄, ~1 ± 10; (NH₃)₅, 37 ± 8. Error limits are 1 SD for the values averaged.

the effect of asymmetry is extremely small (~6 cm⁻¹; see Appendix A). We have not made any corrections for this effect.

d. The Variations in $E_{1/2}^{\text{obsd}}$ that Result from Changes in the Nonbridging Ligands. There are systematic changes in $E_{1/2}(\text{Ru}(\text{NH}_3)_5^{3+,2+})$ that occur when the ligands (L) on the acceptor (M) are altered in L(CN)_{2-n}M(CNRu(NH₃)₅)_n⁽¹⁺²ⁿ⁾⁺ complexes (M = Rh³⁺, Co³⁺, or Cr³⁺). The relative changes (M constant) are characteristic of the nonbridging ligand (Table 7), and they do not vary significantly with ϵ_s^{op} . The most likely origin of these effects is solvational; that is, that the solvation of the D and A centers of these complexes is not entirely independent.⁹⁴ In the CN⁻-bridged complexes these effects are relatively large, comparable to ϵ_s^{op} and relatively easily taken into account since they are independent of M (and ϵ_s^{op}). Such systematic variations of $E_{1/2}$ in D/A complexes when nonbridging ligands are altered may be a more serious problem than has been generally recognized. The studies reported here are unique in that we have been able to correct for such coupled solvational effects by comparing complexes that differ only in their acceptors M.

6. The Observed Contrasts between ϵ_s^{th} and ϵ_s^{op} . In Figure 7 we present observations regarding the correlation of $E_{1/2}(\text{Ru}(\text{NH}_3)_5^{3+,2+})$ with ϵ_s^{op} . The corrections of ϵ_s^{op} for symmetry effects and $E_{1/2}^{\text{obsd}}$ for solvational effects have been described above. The straightforward application of these corrections results in different correlations for complexes with polypyridyl nonbridging ligands than is found for complexes with am(m)ine nonbridging ligands. The extent of this difference depends only on the "correction" for the charge difference between M(II)- and M(III)-centered complexes; for example, for the MMCT excited states of the polypyridyl complexes one would expect appreciable Cr²⁺/polypyridine and CN⁻/Ru(bpy)₂³⁺ charge delocalizations. This should lead to relatively smaller values of r_{ge}^{c} than found for the am(m)ine complexes and thus to

larger values of H_{DA} and ϵ_s ; therefore, eq 23 suggests a steeper slope of the correlation for the polypyridyl complexes, qualitatively as observed in Figure 7. However, it is very unsettling that this approach results in different values for $E_{1/2}^{\text{ref}}$. There is no obvious justification for such a (44 mV) difference. The very similar values of ϵ_s^{corr} for Cr(III)-centered complexes are also difficult to justify in terms of the arguments presented above (which suggest a smaller value of r_{ge}^{c} for Cr(III) complexes with polypyridyl than for those with am(m)ine nonbridging ligands). That these values of ϵ_s are so similar (289 ± 35 cm⁻¹) suggests that such charge delocalization onto nonbridging ligands may not be a major factor in determining r_{ge}^{c} and that the major contributing factors relate to charge delocalization along the D-A axis (see also Cave and Newton^{29b}).

If one imposes the requirement that $E_{1/2}^{\text{ref}}$ be the same for all complexes in this correlation after corrections for differences in solvation, then the "solvational" correction required for the Ru(II) and Fe(II) complexes is $\delta\Delta E_{1/2} \cong 118$ mV (compared to 65 mV based on the pairs of couples in Table 6). Such a value of $\delta\Delta E_{1/2}$ could be entirely a solvational effect, or it could be a combination of solvational differences and variations in r_{ge}^{c} . On the basis of experimental LMCT and MLCT parameters (Tables 2 and 3) we would estimate that there is about 42 mV greater stabilization (ϵ_s^{th}) resulting from charge delocalization in the electron-transfer excited state for the Ru(bpy)₂-centered complexes (i.e., from CN⁻/Ru(III)LMCT) than for the Cr(bpy)₂-centered complexes (i.e., from Cr(II)/CN⁻(MLCT)). Assuming similar ground-state delocalization, this estimate, combined with eq 23, would come close to accounting for the above value of $\delta\Delta E_{1/2}$.⁹⁵ However, this interpretation also implies that the proportionality "constant", *m*, in eq 26 varies from one complex to another (see eq 23 and Discussion section B3). Complexes with less oxidizing Ru(III) centers might be useful in assessing whether this interpretation is correct. The approach in Figure 7b seems to have fewer problems than the approach in Figure 7a.

In principle, one might use $E_{1/2}(\text{Ru}(\text{bpy})_2^{3+,2+})$ to estimate ϵ_s^{th} . In practice it is difficult to account for all the solvational,⁷⁵ entropic,⁹⁶ or other factors contributing to the stabilization of the Ru(bpy)₂³⁺-centered oxidation product and to $E_{1/2}$ for this couple. Many of these factors should disappear when the differences of $E_{1/2}$ are compared for cyano ruthenates (Ru(NH₃)₅³⁺) and cyano rhodates (Rh(NH₃)₅³⁺). The experimental differences in $E_{1/2}(\text{Ru}(\text{bpy})_2^{3+,2+})$ are 90 ± 10 mV for the monoruthenates and 75 ± 10 mV for the bisruthenates (Table 1s).³⁹ The values calculated, based on the correlations in Figure 7b, are 97 and 75 mV, respectively. For this surprisingly good agreement to be meaningful, the $\Delta E_{1/2}$ "correction" above would have to be purely solvational and r_{ge}^{c} would have to be constant through the series of complexes. Such a simple result also

TABLE 8: Electronic Matrix Elements and Stabilization Energies Based on Optical (MM'CT) Spectra

central (MCL)	formal charges of metals (Ru, M, Ru)	H_{DA}^{op}/Ru , $cm^{-1}/10^3$ ^a	ϵ_s^{op} , cm^{-1} ^b	ϵ_s^{th} , cm^{-1} ^c	H_{DA} , $cm^{-1}/10^3$ ^d
Ru(bpy) ₂ ²⁺	(3,2,3)	2.1	297	772	3.4(4.4)
Ru(bpy) ₂ ²⁺	(3,2)	2.1	305	793	3.4(4.4)
Ru(tpy)(bpy) ²⁺	(3,2)	2.1	305	793	3.4(4.4)
Fe(bpy) ₂ ²⁺	(3,2,3)	1.7	240	624	2.7(3.3)
Fe(phen) ₂ ²⁺	(3,2,3)	1.7	248	645	2.7(3.3)
Fe(bpy) ₂ ²⁺	(3,2)	1.9	324	842	3.0(3.7)
Rh(bpy) ₂ ³⁺	(2,3,2)	(1.6) ^e	85	221	2.6 ^e
<i>t</i> -Rh([14]aneN ₄) ³⁺	(2,3,2)	(1.0) ^e	37	96	1.7 ^e
<i>t</i> -Rh(<i>m</i> -Me ₆ [14]aneN ₄) ³⁺	(2,3,2)	(1.8) ^e	37		
<i>t</i> -Co([14]aneN ₄) ³⁺	(2,3,2)	1.1	56	146	1.7
<i>t</i> -Co(<i>m</i> -Me ₆ [14]aneN ₄) ³⁺	(2,3,2)	1.2	76	198	2.0
Cr(bpy) ₂ ³⁺	(2,3,2)	2.0	256	666	3.2
Cr(bpy) ₂ ³⁺	(2,3)	2.3	329	855	3.6
<i>t</i> -Cr([14]aneN ₄) ³⁺	(2,3,2)	2.5	300	780	3.9
<i>t</i> -Cr(<i>m</i> -Me ₆ [14]aneN ₄) ³⁺	(2,3,2)	2.2	244	634	3.5
Cr(NH ₃) ₅ ³⁺	(2,3)	2.4	269	699	3.9

^a From eq 4 with $r_{DA}^c = 5.2$ Å. ^b From eq 20. ^c Based on the $\epsilon_s^{th} = 2.6\epsilon_s^{op}$ or $3.2\epsilon_s^{op}$ for $M_c = Ru(II)$ or $Fe(II)$. ^d $H_{DA} = [\epsilon_s^{th}E_{DA}]^{1/2}$. ^e The absorption on which this is based may have a substantial Ru(II)/CN⁻ MLCT contribution.

seems surprising, and we suspect that there may be a fortuitous cancellation of the factors that stabilize Ru(bpy)₂³⁺ and those that stabilize Ru(bpy)₂²⁺ centered complexes. The alternative view, noted above (i.e., with a nonsolvational component of about 42 mV for both complexes), would suggest $m \approx 3.2$ for Ru(bpy)₂³⁺-centered complexes (compared to $m = 2.6$ for Cr(II)-centered complexes) and leads to $\epsilon_s^{th} \approx 119$ and 92 mV, respectively, for these complexes.

C. The Values of H_{DA} : Results and Comparisons to Models for Electronic Coupling. 1. *Values of H_{DA} .* Our best estimates of values of H_{DA} , based on the correlation in Figure 7b, for several CN⁻-bridged D/A complexes are listed in Table 8. The $d\pi$ -donor/ $d\pi$ -acceptor systems have comparable values of $H_{DA} \approx 3 \times 10^3$ cm⁻¹. Significantly smaller values are obtained for the $d\pi$ -donor/ $d\sigma$ -acceptor complexes $H_{DA} \approx 2 \times 10^3$ cm⁻¹. The smaller values of H_{DA} for the complexes with $d\sigma$ acceptor orbitals is intuitively appealing since one expects relatively poorer σ/π than π/π overlap and since LMCT transitions with σ/π symmetry are generally less intense than those with similar donor and acceptor orbital symmetries.^{70,97,98}

2. *Comparison to D/A Coupling Models.* The infrared spectra reported previously⁴⁰ and the CT spectra discussed above strongly implicate the bridging CN⁻ as a major factor in determining the magnitude of H_{DA} in CN⁻-bridged D/A complexes. The mechanism by which the bridging ligand promotes D/A electronic coupling has been a major concern of our work.

Superexchange models are commonly employed to describe bridging ligand mediated D/A coupling. If we use the spectroscopic MLCT/LMCT parameters in eqs 15 and 16, then the resulting H_{DA}^s are less than 50% of the values in Table 8 even in the most favorable cases, and those parameters predict about a 5-fold lower value of H_{DA}^s for Cr(III)-centered complexes with polypyridyl than with am(m)ine nonbridging ligands. This, combined with our observation of similar values of H_{DA} , suggests less than a 20% contribution of H_{DA}^s to H_{DA} . Another feature of the superexchange model is that, based on eq 17, H_{DA}^s is expected to be a function of the nuclear coordinates (see Figure 8). For our systems this translates into a dependence on E_{DA} ; thus, for $E_{ACT} = E_{DCT} - E_{DA}$ and $E_{DA} \ll E_{DCT}$, eq 15 can be rewritten as in eq 28.

$$H_{DA}^s \cong [(H_{DCT}H_{ACT})/E_{DCT}](1 + E_{DA}/2E_{DCT}) \quad (28)$$

Consequently, for small E_{DA} , H_{DA}^s should increase with in-

creasing E_{DA} . We find no evidence for such behavior. Furthermore, when $E_{DA} \approx E_{DCT}$, eqs 15–17 predict that H_{DA}^s should become very large. It appears that $E_{DA} \approx E_{DCT}$ for the Rh(III)-centered am(m)ine complexes, while $E_{DA} < E_{DCT}$ for their Co(III) analogues, yet comparable, small values of H_{DA} are found for these complexes (Table 8). We infer that eqs 15–17, and the superexchange model that they embody, do not properly describe electronic coupling in the CN⁻-bridged D/A complexes.

The superexchange model does not explicitly take account of effects arising from variations in the relaxation of nuclear coordinates that accompany the delocalization of charge (α_{DCT}^2 or α_{ACT}^2 ; to or from the bridging ligand) in the ground state. It treats the effects of MLCT and LMCT perturbations separately, and these second-order perturbations should in principle be small. Consequently, it is difficult to see how the superexchange approach would be consistent with significant variation of the ground-state properties of the bridging ligand. Yet there are very substantial shifts of the ground-state CN⁻ stretching frequency which correlate with variations in H_{DA} .⁴⁰ As a result of such considerations and the points made above, we have explored the use of a simple, semiclassical vibronic approach to address these issues.^{39c,d,40} This approach in effect treats the D(CN⁻)A interaction as a weak, multicenter bonding interaction in which the MLCT, LMCT, and DACT perturbations mix synergistically to produce stronger D/A coupling than would be generated by the sum of the corresponding superexchange components. The approach is sketched in Appendix B. The stabilization of the ground state due to vibronic coupling is given by eq 29^{39,40} (Appendix B), in which the parameters refer to

$$\epsilon_s^{th} \cong E_{DA}/2 + kx_{min}^2/2 - (1/2)[E_{DA}^2 + 4a^2x_{min}^2 + 4ax_{min}E_{DA} + 4E_{DA}\epsilon_s^{op}]^{1/2} \quad (29)$$

the complex in which no nuclear relaxation has occurred, and $x_{min} \cong (a + 2\alpha_{DA}^o b)/k$, $a \cong 4\alpha_{CT}^o(\lambda_{CT}k/2)^{1/2}$, and $b \cong (\lambda_{DA}k/2)^{1/2}$ (see Appendix B and refs 39–41) lead to the conclusion that $\epsilon_s^{th} > \epsilon_s^{op}$ (in strongly coupled systems with $E_{DA} \gg \lambda_i$, ϵ_s^{op}) whenever $2(\alpha_{CT}^o)^2\lambda_{CT} > (\alpha_{DA}^o)^2\lambda_{DA}$; that is, for the conditions stated one obtains eq 30.

$$\epsilon_s^{th} - \epsilon_s^{op} \cong 2(\alpha_{CT}^o)^2\lambda_{CT} - (\alpha_{DA}^o)^2\lambda_{DA} \quad (30)$$

A rough comparison of eq 30 to experimental parameters can be made for the Cr([14]aneN₄)(CNRu(NH₃)₅)₂⁵⁺ complex (ratios

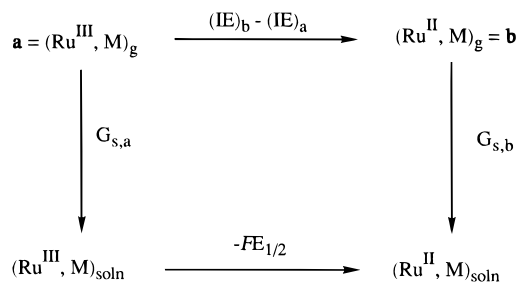
contain numerical values of energies in 10^3 cm^{-1}): (a) $\alpha_{\text{CT}}^{\text{c}}(\text{g}) \approx 2/30 = 0.07$ and $\alpha_{\text{CT}}^{\text{c}}(\text{e}) \approx 2/10 = 0.2$; (b) $\alpha_{\text{DA}}^{\text{c}} \approx 0.5/20 = 0.025$; (c) $\lambda_{\text{CT}} \approx 9 \times 10^3 \text{ cm}^{-1}$; (d) $\lambda_{\text{DA}} \approx 4 \times 10^3 \text{ cm}^{-1}$. These parameters and eq 30 lead to $(\epsilon_s^{\text{th}} - \epsilon_s^{\text{op}}) \approx 350 \text{ cm}^{-1}$, which is comparable to the value of 480 cm^{-1} determined above. Given the gross approximations and a very simple model, this is excellent agreement and good support for the basic elements of the argument.

Conclusions

In this report we have compared two experimental measures of donor–acceptor electronic coupling in CN⁻-bridged transition metal D/A complexes: (a) the oscillator strength of the MM'CT absorption band and (b) variations in the half-wave potentials of the Ru(NH₃)₅2^{3+,2+} couple. This work involved the preparation and study of complexes with five different central metals combined with up to six different nonbridging ligands. This wide range of complexes has allowed experimental comparisons that have demonstrated the importance of solvation effects in the electrochemical studies: (i) changes in nonbridging ligands result in systematic variations in $E_{1/2}$ (e.g., about 10 mV per methyl substituent on an aliphatic nonbridging ligand); (ii) a one unit increase in charge of the central cation results in at least a 50 mV increase in $E_{1/2}$, and possibly as much as 120 mV; and (iii) the variations of $E_{1/2}$ with solvent are approximately equal in magnitude to the solvent variations of the reorganizational energy associated with electron transfer. An empirical correlation $E_{1/2}^{\text{corr}} = 1630 + (1.09 \times 10^{-3})h_{\text{DA}}/r_{\text{DA}}$ (h_{DA} = oscillator strength, $\epsilon_{\text{max}}\Delta\nu_{1/2}$, in $\text{cm}^{-2} \text{ M}^{-1}$; $E_{1/2}$ in mV) can be generated, provided corrections are made for MM'CT degeneracy (or symmetry; in h_{DA}), for solvational differences arising from changes in nonbridging ligands, and for charge (or possibly other) differences that arise when an M(III) central metal is replaced by a M(II) central metal. This implies that the actual stabilization energy of the D/A complex is 2.6 times larger than that calculated from the oscillator strength and the assumption that the effective distances between the centers of charge, r_{ge}^{c} , in the ground and excited states, is equal to the D/A separation, r_{DA} . This single correlation for all the complexes implies $r_{\text{ge}}^{\text{c}} \approx 0.62r_{\text{DA}}$. In view of the fitting procedure used, this may be more correct for M(III)-centered complexes than for Fe(II)- and Ru(II)-centered complexes; for the latter r_{ge}^{c} could be as small as $0.56r_{\text{DA}}$. These inferences are qualitatively consistent with recent electroabsorption studies^{48–52} and indicate that electronic coupling is very strong in the Cr^{III}–(CN⁻)–Ru^{II}, Ru^{II}–(CN⁻)–Ru^{III}, and Fe^{II}–(CN⁻)–Ru^{III} complexes: $H_{\text{DA}} = (3.6 \pm 0.3) \times 10^3$, $(3.4–4.2) \times 10^3$, and $(2.8–3.4) \times 10^3 \text{ cm}^{-1}$, respectively (the ranges for Ru(II)- and Fe(II)-centered complexes are based on uncertainty in r_{ge}^{c} noted above). Electronic coupling is much smaller in Rh(III)- and Co(III)-centered complexes: $H_{\text{DA}} = (2.1 \pm 0.4) \times 10^3$ and $(1.8 \pm 0.2) \times 10^3 \text{ cm}^{-1}$, respectively.⁹⁶

The inferred values of H_{DA} are much larger and behave differently than expected based on spectroscopic parameters and a simple superexchange model. They are reasonably consistent with a simple vibronic model that assumes that D/A electronic coupling varies with the displacement of bridging ligand nuclei and that the displacement of bridging ligand nuclei varies with the amount of charge delocalized to (and from) the bridging ligand from D (to A). The inferred variations of r_{ge}^{c} are qualitatively consistent with perturbational assessment of charge delocalized, but only if charge delocalized onto (or from) the bridging ligand is the dominant factor in determining H_{DA} in these strongly coupled systems.

SCHEME 1



Acknowledgment. We gratefully acknowledge partial support of this research by the Division of Chemical Sciences, Office of Basic Energy Sciences, Office of Energy Research, U.S. Department of Energy. We also acknowledge several useful suggestions from Dr. V. Swayambunathan and discussions with Professor H. B. Schlegel. S.E.M. acknowledges support from the Conselho Nacional de Desenvolvimento Científico e Tecnológico of Brazil.

Appendix A: The Effects of Differential Solvation on $E_{1/2}^{\text{obsd}}$

The free energy of solvation of a cation with net charge Z and effective radius r_{eff} can be approximated by eq A1, where

$$\Delta G_{\text{solv}} \approx -(Z^2/r_{\text{eff}})f \quad (\text{A1})$$

f is a function of the solvent.⁷⁵ The strong dependence on charge type suggests that the mono- and biscyano metalates should have different values of $E_{1/2}^{\text{ref}}$ (note that r_{eff} will also differ), and this seems qualitatively consistent with the negative shifts of $E_{1/2}^{\text{obsd}}$ when the solvent is changed from acetonitrile to water (the more polar solvent tends to stabilize the higher oxidation state). One also expects some differences in $E_{1/2}^{\text{ref}}$ for the series of M(PP)₂^{3+,2+} complexes (M = Cr, Rh, Co) and the M(PP)₂²⁺ complexes (M = Fe, Ru).

The (PP)₂M(CNRu(NH₃)₅)ⁿ⁺ complexes are very asymmetric, and one expects very different solvation of the M(PP)₂ fragment than of the Ru(NH₃)₅ fragment. For example, the difference in solvational contributions to $E_{1/2}$ for the M(bpy)₃^{3+,2+} and Ru(NH₃)₆^{3+,2+} couples has been estimated to be 100 kJ mol^{-1} (about 1 eV).⁷⁵ As a result, the actual charge distribution within the molecule will result in different solvational contributions to values of $E_{1/2}$ measured at the different centers.

It is convenient to discuss the effects of charge delocalization on the electrochemically determined ground-state stabilization energy in terms of the simple free energy cycle in Scheme 1. With reference to Scheme 1, $E_{1/2}^{\text{ref}}$ may be redefined as in eq A2

$$-E_{1/2}^{\text{ref}} = [(IE)_b - (IE)_a + G_{s,b} - G_{s,a}]F \quad (\text{A2})$$

where $(IE)_i$ and $G_{s,i}$ are the ionization energy and solvation energy, respectively, of the i th species and F is Faraday's constant. Then the effects of electronic coupling will appear as corrections to $(IE)_i$, ϵ_s , or as corrections to the solvation energy, $\delta G_{s,i}$. The latter comes about because the donor–acceptor electronic coupling results in some delocalization of electron density and, in effect, a change of charge type from that of the reference state. The fraction of charge delocalized is given by eq A3.² For CT stabilization of Ru(II), the ionization

$$\alpha^2 = [\beta_g/\Delta E_{\text{DA}}]^2 = F\epsilon_s/\Delta E_{\text{DA}} \quad (\text{A3})$$

energy term becomes $(IE)_b - [(IE)_i - F\epsilon_s]$, and the solvational

term $G_{s,b} - [G_{s,a} + \delta G_{s,a}]$, resulting in eq A4. Based on similar

$$E_{1/2}^{\text{obsd}} = E_{1/2}^{\text{ref}} - \epsilon'_s - \delta G_{s,a} F \quad (\text{A4})$$

reasoning the MM'CT coupling stabilizes Ru(III) and results in eq A5. From eq A1 we infer that $\delta G_{s,i}$ can be approximated

$$E_{1/2}^{\text{obsd}} = E_{1/2}^{\text{ref}} - \epsilon'_s - \delta G_{s,b} F \quad (\text{A5})$$

by eq A6, so that $\delta G_{s,i}$ is given to first order by eq A7.

$$\delta G_{s,i} \cong [Z^2 - (Z \pm \alpha^2)^2] / r_{\text{eff}}' \quad (\text{A6})$$

$$|\delta G_{s,i}| \cong 2\alpha^2 G_s / Z \quad (\text{A7})$$

The Ru(NH₃)₅ center is the dominant factor. Substituting into eqs A6 and A7 we obtain eqs A8 and A9, respectively.

$$E_{1/2}^{\text{obsd}}(\text{II}) \cong E_{1/2}^{\text{ref}} + \epsilon_s [1 - \Delta G_s / \Delta E_{\text{DA}}] F \quad (\text{A8})$$

$$E_{1/2}^{\text{obsd}}(\text{III}) \cong E_{1/2}^{\text{ref}} - \epsilon_s [1 + 0.66 \Delta G_s / \Delta E_{\text{DA}}] F \quad (\text{A9})$$

Thus differential solvational effects, which arise from delocalization of charge, result in an intrinsic redox asymmetry in condensed-phase measurements. It is difficult to assess the magnitude of ΔG_s for the systems considered here. Arguments presented in the text suggest that a reasonable approximation is $\Delta G_s \approx -\lambda_s$. With this approximation the differential solvational contributions amount to less than 10% of ϵ_s^{th} in the systems considered here. Richardson's estimates for the isolated couples suggest an extreme upper limit of $\Delta G_s \cong 100 \text{ kJ mol}^{-1}$ (in water) and differential solvational contributions in the range 30–50% of ϵ_s for Ru or Cr central metals. These effects have the same sign independent of charge type, and only a small fraction can contribute to the slopes in Figure 7.

The arguments in the preceding paragraphs are based on the assumption that the total effect of differential solvation is localized on the pentaamine moiety. If the central metal contributes as well, then eq A8 needs to be modified as in eq A10, where superscripts a and p refer to the ammine and

$$E_{1/2}^{\text{obsd}}(\text{II}) \cong E_{1/2}^{\text{ref}} + \epsilon_s [1 - \Delta G_s^a / \Delta E_{\text{DA}} + 0.66 \Delta G_s^p / \Delta E_{\text{DA}}] \quad (\text{A10})$$

polypyridyl moieties. If we set $\Delta G_s^a \cong \lambda_s^a (\sim 4 \times 10^3 \text{ cm}^{-1})$ and $\Delta G_s^p \cong 0.5 \Delta G_s^a$, then eq A10 may be rewritten as in eq A11. Substituting $h\nu_{\text{max}}(\text{MM}'\text{CT})$ for ΔE_{DA} and $\lambda_{sa} \approx 4 \times$

$$E_{1/2}^{\text{obsd}}(\text{III}) \cong E_{1/2}^{\text{ref}} - \epsilon_s [1 + 0.66 \lambda_s^a / \Delta E_{\text{DA}} - \lambda_s^a / 2 \Delta E_{\text{DA}}] \quad (\text{A11})$$

10^3 cm^{-1} , we find that the correction terms are -66 cm^{-1} for Cr(III) and -72 cm^{-1} for Ru(II) centered complexes. The difference of 6 cm^{-1} is well within estimated error limits.

Appendix B: A Simple Semiclassical Vibronic Model for D/A Coupling

1. Some General Considerations of Metal-Bridging Ligand Interactions in M(CNRu(NH₃)₅)ⁿ⁺ Complexes. The electronic structures of the cyanide-bridged transition metal complexes are relatively complex. To minimize the complexities, we will confine the discussion to simple D⁻(BL)A complexes, such as the monoruthenates of this study. Since we wanted to develop a model in which the key parameters were (in principle) experimentally accessible, we have largely focused on the

MM'CT states, and on the LMCT and MLCT states involving the bridging ligand. We do not include the charge-transfer states involving the polypyridyl ligands. To simplify this discussion, we will assume that these perturbations are either small or nearly constant (e.g., contributions to $E_{1/2}^{\text{ref}}$) through the series of compounds.

The microsymmetry at the Ru(NH₃)₅ center of the monometalates is very close to C_{4v} , so two of the Ru d π orbitals will be nearly degenerate; that is, the d π orbitals can be treated as subsets of e and b₂ symmetry. For Ru(NH₃)₅³⁺ moieties, local CT interactions will tend to favor placing the hole in the e subset, since $\epsilon_L > \epsilon_M$, for the respective LMCT and MLCT stabilization energies designated by L and M. The site symmetry of the central atom of the M(bpy)₂(CN)₂ moieties is (in the bisruthenates) C₂, and there is no degeneracy among the d π orbitals of M. Although there may be some differences in their intensities, this will lead to the convolution of several components in the MM'CT absorption bands of M^{II}CN(Ru^{III})₂ (M = Ru or Fe) complexes and of the Cr^{III}CN(Ru^{II})₂ complexes. The symmetry is lower (C_s) in the monometalates so that selection rule issues, discussed above, are not a problem. The MM'CT absorption bandwidths of these complexes are 30–50% larger than expected on the basis of electron-transfer reorganizational energies, $\lambda_{\text{DA}} \approx 4 \times 10^3 \text{ cm}^{-1}$ for Ru(II)/Cr(III), Ru(II)/Ru(III), and Ru(III)/Fe(II) complexes (see Results section), and a semiclassical analysis of bandwidth.^{3,5,99} The relatively large bandwidths and the nearly Gaussian band shapes are consistent with the convolution of several components which differ little in energy.

The general trends in behavior are most simply discussed in terms of a Hückel-like analysis of the π interactions in a linear, four-orbital–four-atom system. We consider first a symmetric M₁–C₁≡C₂–M₂ species. Since there will generally be a large energy difference between the d π and the p(C) orbitals, we will consider only the respective symmetric and antisymmetric combinations: Φ_s and Φ_a for M₁ and M₂ and Φ_π and Φ_{π^*} for C₁ and C₂. The molecular orbital combinations are given by eqs B1 and the resulting orbital energies are given in eqs B2

$$\left. \begin{aligned} \psi_1(1 + \lambda^2)^{1/2} &= \Phi_\pi + \lambda \Phi_s \\ \psi_2(1 + \lambda^{*2})^{1/2} &= -\lambda^* \Phi_\pi + \Phi_s \\ \psi_3(1 + \gamma^{*2})^{1/2} &= \Phi_{\pi^*} - \gamma^* \Phi_a \\ \psi_4(1 + \gamma^2)^{1/2} &= \gamma \Phi_{\pi^*} + \Phi_a \end{aligned} \right\} \quad (\text{B1})$$

$$\left. \begin{aligned} \epsilon_1 &\cong \alpha_\pi + \beta_\pi^2 / (\alpha_\pi - \alpha_s) \\ \epsilon_2 &\cong \alpha_s - \beta_\pi^2 / (\alpha_\pi - \alpha_s) \\ \epsilon_3 &\cong \alpha_s - \beta_{\pi^*}^2 / (\alpha_{\pi^*} - \alpha_a) \\ \epsilon_4 &\cong \alpha_{\pi^*} + \beta_{\pi^*}^2 / (\alpha_{\pi^*} - \alpha_a) \end{aligned} \right\} \quad (\text{B2})$$

for first-order perturbational mixing. In eqs B2, the $\alpha_i = \langle \Phi_i | H | \Phi_i \rangle$, $\beta_{\pi^*} = \langle \Phi_{\pi^*} | H | \Phi_a \rangle$ and $\beta_\pi = \langle \Phi_\pi | H | \Phi_s \rangle$, in the limit that the overlap integrals are small; for nonnegligible overlap, $\beta_{ij} = \langle \Phi_i | H | \Phi_j \rangle - S_{ij} E_k$ ($k = i$ or j as appropriate). Note that the symmetry-allowed orbital mixings in a one-electron limit correspond to perturbational mixings of bridging ligand and metal orbitals, LMCT with d π for the Φ_π / Φ_s mixing and MLCT with d π^* for Φ_{π^*} / Φ_a . The symmetric five-electron system is necessarily delocalized. When there are MLCT and LMCT transitions involving the bridging ligand, the antisymmetric and symmetric combinations of donor/acceptor metal electronic states will differ in energy. The splitting energy is approximately $2H_{\text{GE}} \cong (\epsilon_L^* + \epsilon_M^*)$, in which the ϵ_i^* is the one-electron stabilization energies resulting from local LMCT and MLCT couplings, respectively, and for the nuclear coordinates of the symmetrical system (denoted by the asterisk).

To the degree that the ϵ_i^* are significant in magnitude, the donor and acceptor states cannot be degenerate in the symmetry-adapted system (note that the symmetry-adapted system corresponds to the “transition state” in the usual analysis of electron-transfer systems). The same basic point has been made in Peipho’s pseudo-Jahn–Teller treatment of the Creutz–Taube ion³⁵ and in a treatment of classical inner-sphere electron-transfer reactions.⁴¹

2. A Vibronic Model for Donor–Acceptor Coupling. *a. Definitions and General Approach.* The argument outlined above is a “four-state” approach: (a) electron localized on the donor in the unperturbed ground state (D); (b) electron localized on the acceptor (A); (c) MLCT; and (d) LMCT excited states. To deal with this problem in a simple way, we first allow for local MLCT and LMCT interactions by means of standard first-order perturbational corrections of the electron transfer state (D and A) potential energies, and we then allow for the D/A coupling perturbation using a 2×2 secular determinant. The net result of the several possible first-order CT interactions will be to alter the potential energies of the ground (subscript “g”) and excited (subscript “e”) electron-transfer states as indicated in eqs B3,

$$\begin{aligned} V_g &= V_g^\circ - \epsilon_L - \epsilon_M - \epsilon_{DA} + k_g x^2/2 \\ V_e &= V_e^\circ - \epsilon_L' - \epsilon_M' + \epsilon_{DA} + k_e x^2/2 \end{aligned} \quad (\text{B3})$$

where the V_i° are PEs in the absence of any CT interactions, the ϵ_i and ϵ_i' are local charge-transfer stabilization energies (L for ligand-to-metal charge transfer; M for metal-to-ligand charge transfer) for the ground and excited states, respectively, and $\epsilon_{DA} = \beta_{DA}^2/\Delta E_{DA}$ is the stabilization energy arising from direct D/A coupling. In general the $\epsilon_{ij} = H_{ij}^2/E_{ij}$ are functions of the electron-transfer coordinate, x . This dependence can be expressed in terms of a first-order Taylor’s series expansion around $x = 0$, as in eq B4. One expects both β_i and ϵ_i for the local CT

$$\epsilon_{ij} \cong \epsilon_{ij}^\circ + [(\partial\epsilon_{ij}/\partial x)_{x=0}]x \quad (\text{B4})$$

interactions to vary with x . If $G_i^\circ \cong [E_{ij}^\circ + k_{ij}(x - x_{ij}^\circ)^2/2]$ and if $\beta = H_{ij} \cong H_{ij}^\circ + a_{ij}x$, then ϵ_{ij} may be expressed as in eq B5, where $\alpha_{ij} = (H_{ij}/E_{ij})$, $\lambda_{ij} = k_{ij}(x^\circ)^2/2$, and we have set $a \cong r(k_{ij}\lambda_{ij}/2)$ (see the following section). The signs of the correction terms in eq B5

$$\begin{aligned} \epsilon_{ij} &\cong \epsilon_{ij}^\circ + 2\alpha_{ij}a_{ij}x + \epsilon_{ij}k_{ij}x_{ij}^\circ/E_{ij} \\ &\cong \epsilon_{ij}^\circ + 2(\alpha_{ij} + \alpha_{ij}^2)x\sqrt{k_{ij}\lambda_{ij}^2} \end{aligned} \quad (\text{B5})$$

will be different for the contributions to the ground and excited electron-transfer states, so that the result in eq B5 may be summarized by $\epsilon_{ij} \cong [\epsilon_{ij}^\circ \pm A_{ij}x]$.

b. The Symmetrical Limit in the Absence of CT Coupling to or from the Bridging Ligand: A Connection to Standard Electron Transfer Formalisms. In the symmetrical limit $V_g^\circ = V_e^\circ = V^\circ$, and in the absence of CT coupling with the bridging ligand (i.e., for $\epsilon_L = \epsilon_M = 0$), and assuming a coupling matrix element $H_{ge} = H_{DA}^\circ + bx$, the roots of the secular equation are given by $\epsilon_\pm = \pm(H_{DA}^\circ + bx)$. Substitution into eq B6, with $\epsilon_{ij} = \epsilon_{ij}' = 0$, results in ground-state PE minima at $x_m = \pm b/k$ and potential energies at x_m are given by eq B6 (assuming $k_g = k_e$).

$$V_g(x_m) \cong V^\circ - H_{DA}^\circ - b^2/2k \quad (\text{B6})$$

$$V_e(x_m) \cong V^\circ + H_{DA}^\circ + 3b^2/2k$$

For the limit in which $|H_{DA}^\circ| \ll b^2/2k$, these equations can be

compared to the classical electron-transfer limit,^{2–4,42} in which $\Delta V(x_m) = \lambda_{DA}$, where λ_{DA} is the nuclear reorganizational energy associated with the D/A electron-transfer process. Thus, $b \cong [\lambda_{DA}k/2]^{1/2}$.

3. The Symmetrical Limit When the Bridging Ligand is CT Coupled to the Donor and/or Acceptor. For simplicity we will treat this as an equivalent three-state problem, for which we assume that V_e and V_g are not dependent on x in the absence of D/A coupling and that $H_{ge} = H_{DA}^\circ + bx$. This results in the PJT limit discussed by Bersuker.⁹⁰ In this limit, the intrinsic splitting of the symmetry adapted D/A states, discussed in a preceding section, is taken as the initial condition so that $\Delta V \cong \epsilon_{CT}^\circ = (\epsilon_M^\circ + \epsilon_L^\circ) = 2H_{CT}^\circ$. If we again assume that $H_{DA}^\circ \cong 0$, then the secular equation has the PJT form⁷⁹ and its roots are given by $\epsilon_\pm = \pm [(H_{CT}^\circ)^2 + b^2x^2]^{1/2}$. If ϵ_{CT}° is very large, so that $(H_{CT}^\circ)^2 \gg b^2x^2$, then there is a single PE minimum and a relatively large bond order for the D–BL bond and/or the BL–A bond (see the previous discussion). A double-minimum situation can only result if H_{CT}° is small (thus, approaching the limit in section 2, above) or if λ_{DA} is relatively large. The PE minima occur for $x_m \cong \pm(b/k)(1 - H_{CT}^{\circ 2}k^2/2b^4)$, and the first-order corrections to the potential energy are of the form given by eq B6, but substituting H_{CT}° for H_{DA}° .

A more appropriate model for this limit is obtained by defining the PE functions for the equivalent three-state problem as in eq B7 and again setting $\Delta V^\circ = \epsilon_{CT}^\circ = 2H_{CT}^\circ$. The form of

$$\begin{aligned} V_g &\cong V_g^\circ - A'x + kx^2/2 \\ V_e &\cong V_e^\circ + A'x + kx^2/2 \end{aligned} \quad (\text{B7})$$

the coefficient A' appropriate for this limit requires some comment. A displacement along the coordinate x in eq B7 corresponds to the delocalization of charge in nearest neighbor CT interactions. This will increase the stabilization energy, ϵ_{CT} , only if the D–BL and/or BL–A bond orders are incrementally increased as the bond order in the bridging ligand is decreased; that is, the competition between charge localizing and delocalizing factors, discussed above, should appear in the definition of A' , and the result should decrease the value of A' if λ_{DA} is sufficiently large compared to λ_{CT} . For small corrections, we can treat the decrease in A' in terms of an attenuation factor, f ; i.e., $A' = A''f$, where A'' is given by eq B5. Recalling that we are dealing with incremental changes in ϵ_{CT} , an appropriate expression would be $f \cong [(\alpha_{CT}^\circ)^2\lambda_{CT} - s(\alpha_{DA}^\circ)^2\lambda_{DA}]/(\alpha_{CT}^\circ)^2\lambda_{CT}$, where s is a scale factor, scaling the ϵ_{DA} corrections to be appropriate for ϵ_{CT} ; we take $s \cong \Delta E_{DA}/E_{CT}$. These expressions and parameters for the RuCNRu complexes described in this report indicate that $f \approx 0.9$ for these complexes. Consequently, we shall set $A' \cong 2\alpha_{CT}^\circ[k_{CT}k_{CT}\lambda_{CT}/2]^{1/2}$ in the remainder of this discussion.

The resulting secular equation has roots given by eq B8. For

$$\epsilon_\pm = \pm[(H_{CT}^\circ + A'x)^2 + (H_{DA}^\circ + bx)^2]^{1/2} \quad (\text{B8})$$

our purposes it is sufficient to consider the special case in which $\lambda_{DA} \ll \lambda_{CT}$, $H_{DA}^\circ \approx H_{CT}^\circ$, $b \approx 0$, and $|H_{CT}^\circ| > |A'x|$. For this example, $\epsilon_\pm \cong \pm(H\sqrt{2} + A'x\sqrt{2})$, so that the single, displaced ground state PE minimum is given by eq B9. As before, a

$$(V_g)_m \approx V^\circ - H_{CT}^\circ\sqrt{2} - \alpha_{CT}^2\lambda_{CT}/2 \quad (\text{B9})$$

double-minimum solution is possible only if $(H_{CT}^\circ + A'x)^2 < (H_{DA}^\circ + bx)^2$. The important new feature of eq B9 is that the vibronic coupling can result in stabilization of the ground state

beyond the stabilization expected based on optical absorption. Thus, the matrix element for optical absorption is $H_{DA} = (H_{DA}^0 + bx)$ so that the expression for ground-state stabilization, based on eq B8, can be written as in eq B10.

$$\epsilon_s^{\text{th}} \cong [(H_{CT}^0 + A'x)^2 + (H_{DA}^0)^2]^{1/2} \quad (\text{B10})$$

4. Unsymmetrical Donor–Acceptor Systems with CT Coupling with the Bridging Ligand. This is the limit most pertinent to the cyano-bridged complexes of concern here. In this limit, and using the three-state approximation introduced above, we can set $\Delta V^0 = \Delta E_{DA} + 2\epsilon_{CT}^0 = \Delta$ (see eq B7). It is useful to describe the PE functions as in eq 16. With this definition, the procedures described above result in eq B11 (assuming the $k_{CT} = k_{DA}$).

$$V_g' = -A'x + kx^2/2$$

$$V_e' = \Delta + A'x + kx^2/2 \quad (\text{B11})$$

Since the vibronic matrix element is $H_{DA} = (H_{DA}^0 + bx)$, the resulting secular equation gives rise to eq 29 for the ground-state stabilization energy.

Supporting Information Available: Tables 1s, 2s, and 3s and Figures 1s–7s (13 pages). Ordering information is available on any current masthead page.

References and Notes

- Barbara, P.; Meyer, T. J.; Ratner, M. J. *Phys. Chem.* **1996**, *100*, 13148.
- Mulliken, R. S.; Person, W. B. *Molecular Complexes*; Wiley-Interscience: New York, 1967.
- (a) Hush, N. S. *Electrochim. Acta* **1968**, *13*, 1005. (b) Hush, N. S. *Prog. Inorg. Chem.* **1968**.
- Newton, M. D. *Chem. Rev.* **1991**, *91*, 767.
- Creutz, C. *Prog. Inorg. Chem.* **1983**, *30*, 1.
- Richardson, D. E.; Taube, H. *Coord. Chem. Rev.* **1984**, *60*, 107.
- Haim, A. *Comments Inorg. Chem.* **1984**, *4*, 113.
- Endicott, J. F. *Acc. Chem. Res.* **1988**, *21*, 59.
- Billing, R.; Rehorick, D.; Hennig, H. *Top. Curr. Chem.* **1970**, *152*.
- Crutchley, R. J. *Adv. Inorg. Chem.* **1994**, *41*, 273.
- Ward, M. D. *Chem. Soc. Rev.* **1995**, *21*.
- Fackler, J. P. In *Encyclopedia of Inorganic Chemistry*; King, R. B., Ed.; Wiley: London, 1994; Vol. 5, p 2270.
- Cannon, R. D. *Electron Transfer*; Butterworth: London, 1980.
- Endicott, J. F. In *Encyclopedia of Inorganic Chemistry*; King, R. B., Ed.; Wiley: London, 1994.
- Electron Transfer in Biology and the Solid State*; Johnson, M. K.; King, R. B.; Kurtz, Jr., D. M.; Kuttal, C.; Morton, M. L.; Scott, R. A., Eds.; ACS Advances in Chemistry Series 226; American Chemical Society: Washington, DC, 1980.
- Fox, M. A.; Channon, M., Eds. *Photoinduced Electron Transfer*; Elsevier: Amsterdam: 1988, Parts A–D.
- Newton, M. D.; Sutin, N. *Annu. Rev. Phys. Chem.* **1988**, *35*, 437.
- Weaver, M. J. *Adv. Rev.* **1992**, *92*, 463.
- Wasielowski, M. R. *Chem. Rev.* **1993**, *92*, 435.
- Jordan, K. D.; Padden-Row, M. N. *Chem. Rev.* **1992**, *92*, 395.
- Isied, S. S.; Ogawa, M. Y.; Wishart, J. F. *Chem. Rev.* **1992**, *92*, 381.
- Winkler, R. J.; Gray, H. E. *Chem. Rev.* **1992**, *92*, 369.
- Masuda, A.; Masuda, Y.; Fukuda, Y. *J. Phys. Chem.* **1997**, *101*, 2245.
- Tolbert, L. M.; Zhao, X. *J. Am. Chem. Soc.* **1997**, *117*, 3253.
- Kestner, N.; Logan, J.; Jortner, J. *J. Phys. Chem.* **1974**, *78*, 2148.
- Beratan, D. N.; Onuchic, J. N.; Betts, J. N.; Bowler, B. E.; Gray, H. B. *J. Am. Chem. Soc.* **1990**, *112*, 7915.
- Lopez-Castillo, J.-M.; Jay-Gerin, J.-P. *J. Phys. Chem.* **1996**, *100*, 14289.
- Reimers, J. R.; Hush, N. S. *Chem. Phys.* **1996**, *208*, 177.
- (a) Cave, R. J.; Newton, M. D. *Chem. Phys. Lett.* **1996**, *249*, 15. (b) Cave, R. J.; Newton, M. D.; Kumar, K.; Zimmet, M. D. *J. Phys. Chem.* **1995**, *99*, 17501.
- McConnell, H. M. *J. Chem. Phys.* **1961**, *35*, 508.
- Kuznetsov, A. M. *Charge Transfer in Physics, Chemistry and Biology*; Gordon and Breach: Reading, U.K., 1995.
- (a) Zhang, L.-T.; Ko, J.; Ondrechen, M. J. *J. Phys. Chem.* **1989**, *93*, 3030. (b) Ondrechen, M. J.; Gozashiti, S.; Zhang, L.-T.; Zhou, F. In *Electron Transfer in Biology and the Solid State*; Johnson, M. K.; King, R. B.; Kurtz, D. M.; Kuttal, C.; Norton, M. L.; Scott, R. A., Eds.; ACS Advances in Chemistry Series No. 226, American Chemical Society: Washington, DC, 1990; p 225.
- Ferretti, A.; Lami, A.; Ondrechen, M. J.; Villani, G. *J. Phys. Chem.* **1995**, *99*, 10484.
- Peipho, S. B.; Krausz, E. R.; Schatz, P. N. *J. Am. Chem. Soc.* **1978**, *100*, 2996.
- (a) Piepho, S. B. *J. Am. Chem. Soc.* **1988**, *110*, 6319. (b) Piepho, S. B. *J. Am. Chem. Soc.* **1990**, *112*, 4197.
- Bixon, M.; Jortner, J.; Verhoeven, J. W. *J. Am. Chem. Soc.* **1994**, *116*, 7349.
- Marcus, R. A. *Annu. Rev. Phys. Chem.* **1965**, *15*, 155.
- Calzado, C. J.; Sanz, J. F.; Costello, O.; Caballo, R. *J. Phys. Chem.* **1997**, *101*, 1716.
- (a) Endicott, J. F.; Song, X.; Watzky, M. A. *Chem. Phys.* **1993**, *176*, 427. (b) Endicott, J. F.; Song, X.; Watzky, M. A.; Buranda, T. *Photochem. Photobiol. A: Chem.* **1994**, *92*, 181. (c) Endicott, J. F.; Watzky, M. A.; Song, X.; Buranda, T. *Coord. Chem. Rev.* **1997**, *159*, 295. (d) Endicott, J. F.; Watzky, M. A.; Macatangay, A. V.; Mazzetto, S. E.; Song, X.; Buranda, T. In *Electron and Ion Transport in Condensed Media*; Kornyshev, A., Ed.; World Scientific Publishers: Singapore, in press.
- Watzky, M. A.; Endicott, J. F.; Song, X.; Lei, Y.; Macatangay, A. *Inorg. Chem.* **1996**, *35*, 3463.
- Schwarz, C. L.; Endicott, J. F. *Inorg. Chem.* **1995**, *34*, 4572.
- Marcus, R. A. *J. Phys. Chem.* **1989**, *93*, 3078.
- (a) Endicott, J. F.; Ramasami, T.; Gaswick, D. C.; Tamilarasan, R.; Heeg, M. J.; Brubaker, G. R.; Pyke, S. C. *J. Am. Chem. Soc.* **1983**, *105*, 5301. (b) Ramasami, T.; Endicott, J. F. *J. Phys. Chem.* **1986**, *90*, 3740.
- (a) de la Rosa, R.; Chang, P. J.; Salaymeth, F.; Curtis, J. C. *Inorg. Chem.* **1985**, *24*, 4229. (b) Salaymeth, F.; Berhau, S.; Yusof, R.; de la Rosa, R.; Fung, E. Y.; Matamoros, R.; Law, K. W.; Zheng, Q.; Kober, E. M.; Curtis, J. C. *Inorg. Chem.* **1993**, *32*, 3895.
- (a) Mines, G. A.; Roberts, J. A.; Hupp, J. T. *Inorg. Chem.* **1992**, *31*, 125. (b) Mines, G. A.; Roberts, J. A.; Bebel, J. C.; Absi, M. P.; Hupp, J. T. *J. Am. Chem. Soc.* **1992**, *114*, 7957.
- (a) Saleh, A. A.; Crutchley, R. J. *Inorg. Chem.* **1990**, *29*, 2132. (b) Evans, C. E. B.; Ducharme, D.; Naklicki, M. L.; Crutchley, R. J. *Inorg. Chem.* **1995**, *34*, 1350.
- (a) Gamelin, D. R.; Bominaar, E. L.; Mathonière, C.; Kirk, M. L.; Girerd, J.-J.; Solomon, E. I. *Inorg. Chem.* **1996**, *35*, 4323. (b) Gamelin, D. R.; Bominaar, E. L.; Kirk, M. L.; Wieghardt, K.; Solomon, E. I. *J. Am. Chem. Soc.* **1996**, *118*, 8085.
- Creutz, C.; Newton, M. D.; Sutin, N. *Photochem. Photobiol. A: Chem.* **1994**, *82*, 47.
- Shin, Y. K.; Brunschwig, B. S.; Creutz, C.; Sutin, N. *J. Phys. Chem.* **1996**, *100*, 8157.
- Karki, L.; Lu, H. P.; Hupp, J. T. *J. Phys. Chem.* **1996**, *100*, 15637.
- Reimers, J. R.; Hush, N. S. *J. Phys. Chem.* **1991**, *95*, 9773.
- (a) Oh, D. H.; Boxer, S. G. *J. Am. Chem. Soc.* **1990**, *112*, 8161. (b) Oh, D. H.; Sano, M.; Boxer, S. G. *J. Am. Chem. Soc.* **1991**, *113*, 6880.
- Ligand abbreviations: [14]aneN₄ = cyclam = 1,4,8,11-tetraazacyclotetradecane; [15]aneN₄ = 1,4,8,12-tetraazacyclopentadecane; ms-(5,12)-Me₆[14]aneN₄ = teta = 5,12-meso-5,7,7,12,14,14-hexamethyl-1,4,8,11-tetraazacyclotetradecane.
- Lessard, R. B.; Heeg, M. J.; Buranda, T.; Perkovic, M. W.; Schwarz, C. L.; Rudong, Y.; Endicott, J. F. *Inorg. Chem.* **1992**, *31*, 3091.
- Kane-Maguire, N. A. P.; Miller, P. K.; Trzupke, L. S. *Inorg. Chim. Acta.* **1983**, *76*, L179.
- Whimp, P. O.; Curtis, N. F. *J. Chem. Soc. A* **1996**, 867, 1821.
- Curtis, N. F.; Cook, D. F. *J. Chem. Soc., Dalton Trans.* **1972**, 691.
- Yung, K. *Inorg. Synth.* **1980**, *20*, 111.
- Ricciardi, P.; Zinato, E. *Inorg. Chem.* **1980**, *19*, 853.
- Skibsted, L. H.; Ford, P. C. *Inorg. Chem.* **1983**, *22*, 2749.
- (a) Bignozzi, C. A.; Roffia, S.; Scandola, F. *J. Am. Chem. Soc.* **1985**, *107*, 1644. (b) Bignozzi, C. A.; Scandola, F. *Inorg. Chem.* **1984**, *23*, 1540. (c) Roffia, S.; Paradisi, C.; Bignozzi, C. A. *Electroanal. Chem. Interfacial Electrochem.* **1986**, *200*, 105. (d) Scandola, F.; Bignozzi, C. A. In *Supramol. Photochemistry*; Balzani, V., Ed.; NATO ASI Series C 214; Reidel: Dordrecht, The Netherlands; 1987; p 121. (e) Scandola, F.; Roffia, S.; Paradisi, C.; Bignozzi, C. A. *Inorg. Chem.* **1988**, *27*, 1108.
- Macatangay, A. V.; Watzky, M. A.; Mazzetto, S. E.; Endicott, J. F. Work in progress.
- Bard, A. J.; Faulkner, L. R. *Electrochemical Methods: Fundamentals and Applications*; Wiley-Interscience: New York, 1980.
- Watzky, M. A.; Song, X.; Endicott, J. F. *Inorg. Chim. Acta* **1994**, *226*, 109.
- Supporting Information.
- Forlano, P.; Baraldo, L. M.; Olabe, J. A.; Della Vedova, C. O. *Inorg. Chim. Acta* **1994**, *223*, 37.
- Karki, L.; Hupp, J. T. *J. Am. Chem. Soc.* **1997**, *119*, 4070.
- We have prepared a [Ru(NH₃)₅]₂CN⁴⁺ species for which the molar absorptivity is 4.2 × 10³ M⁻¹ cm⁻¹ for a broad ($\Delta\nu_{1/2} = 5.6 \times 10^3$ cm⁻¹)

absorption at 890 nm. (b) Watzky, M. A., Ph.D. Dissertation, Wayne State University, 1994.

- (69) Vogler, A.; Kunkley, H. *Inorg. Chim. Acta* **1981**, *53*, 205.
(70) Lever, A. P. B. *Inorganic Electronic Spectroscopy*, 2nd ed.; Elsevier: New York, 1984.
(71) (a) Alexander, J. J.; Gray, H. B. *J. Am. Chem. Soc.* **1968**, *90*, 4260. (b) Gray, H. B.; Beach, N. A. *J. Am. Chem. Soc.* **1963**, *85*, 2922. (c) Guterman, D. F.; Gray, H. B. *Inorg. Chem.* **1972**, *11*, 1727. (d) Alexander, J. J.; Gray, H. B. *Coord. Chem. Rev.* **1967**, *2*, 29.
(72) For the Ru(CN)₆³⁻⁴⁻ couple $E_{1/2} \cong 0.92$ V.⁷³ If the reorganizational energy differences are negligible, and for the lowest energy LMCT band of Ru(CN)₆³⁻ at 21.8×10^3 cm⁻¹, one would predict $h\nu_{\max} \approx 27 \times 10^3$ cm⁻¹ for CN⁻ → Ru(II) LMCT band of (NH₃)₅RuCN²⁺ (using $h\nu_{\max} \cong \Delta E_{1/2} + \lambda_{\text{reorg}}$). For Ru(CN)₆⁴⁻ the lowest MLCT transition is reported to be at 48.5×10^3 cm⁻¹, which would imply that $h\nu_{\max} \approx 43 \times 10^3$ cm⁻¹ for the lowest energy Ru(II) → CN⁻ LMCT band of (NH₃)₅RuCN⁺.
(73) McCartney, D. *Inorg. Chem.* **1991**, *30*, 3337.
(74) Shaw, J.; Everett, G. W. *Inorg. Chem.* **1985**, *24*, 1917.
(75) Richardson, D. E. *Inorg. Chem.* **1990**, *29*, 3213.
(76) The stabilization energy of the ground state and destabilization energy of the CT excited state do not enter into eq 2 because the perturbational horizontal displacement of the ground-state PE minimum results in the cancellation of these contributions (we are grateful to Dr. M. D. Newton for bringing this point to our attention).
(77) For related arguments see: (a) Lever, A. B. P. *Inorg. Chem.* **1990**, *29*, 1271. (b) *ibid.* **1991**, *30*, 1980. (c) Masui, H.; Lever, A. B. P. *Inorg. Chem.* **1993**, *32*, 2199.
(78) Our spectral deconvolutions have generally indicated that there are two components of the Ru(NH₃)₅²⁺ → bpy MLCT "transition", the second at about 4×10^3 cm⁻¹ higher energy than the first. These can possibly be assigned as the symmetric and antisymmetric components of the transition (two identical bpy ligands in a molecule of C₂ symmetry).^{79,80} For simplicity, only one component is considered here. There could also be a weak, high-energy MM'CT component as noted in Figure 5.
(79) Zwickel, A. M.; Creutz, C. *Inorg. Chem.* **1969**, *10*, 2395.
(80) Parker, W. L.; Crosby, G. A. *Int. J. Quantum Chem.* **1991**, *39*, 299.
(81) We have also observed weak absorption bands at about 430–460 nm in some of the M(MCL)(CNRu(NH₃)₅)₂⁷⁺ complexes (M = Co³⁺ and Cr³⁺). These appear to be the central metal d–d absorptions, and they are shifted 20–25 nm to longer wavelength than to the parent M(MCL)(CN)₂⁺ d–d absorptions for both Co³⁺ and Cr³⁺. This would correspond to about a 5% decrease in D_q(CN⁻) upon metalation. The absorptivities of these bands are about 4 times larger in the ruthenates than in the parent dicyano complexes.
(82) (a) Doorn, S. K.; Stoutland, P. O.; Dyer, R. B.; Woodruff, W. H. *J. Am. Chem. Soc.* **1992**, *114*, 3133. (b) Doorn, S. K.; Dyer, R. B.; Stoutland, P. O.; Woodruff, W. H. *J. Am. Chem. Soc.* **1993**, *115*, 6398.
(83) (a) Walker, G. L.; Barbara, P. F.; Doorn, S. K.; Hupp, J. T. *J. Phys. Chem.* **1991**, *95*, 5712. (b) Tominaggi, K.; Kliner, D. A. V.; Johnosn, A.

E.; Levinger, N. E.; Barbara, P. F. *J. Phys. Chem.* **1995**, *99*, 2609.

- (84) Buranda, T.; Lei, Y.; Endicott, J. F. *J. Am. Chem. Soc.* **1992**, *114*, 135.
(85) Ponce, A.; Bachrach, M.; Farmer, P. J.; Winkler, J. R. *Inorg. Chim. Acta* **1996**, *243*, 135.
(86) Endicott, J. F.; Lessard, R. B.; Lei, Y.; Ryu, C. K. In *Photoinduced Charge Separation and Energy Migration in Supramolecular Species*; Balzani, V., Ed.; NATO ASI C-series; Reidel: Dordrecht, 1987.
(87) Nakamoto, K. *Infrared and Raman Spectra of Inorganic and Coordination Compounds*, 4th ed.; Wiley: New York, 1986.
(88) For simplicity we label the electronic states by the center at which the charge is predominantly localized.
(89) Reimers, J. R.; Hush, N. S. *Photochem. Photobiol. A: Chem.* **1994**, *82*, 31.
(90) Bersuker, I. B. *The Jahn–Teller Effect and Vibronic Interactions in Modern Chemistry*, Plenum: New York, 1984.
(91) Fischer, G. *Vibronic Coupling*; Academic: New York, 1984.
(92) Ballhausen, C. J. In *Vibronic Processes in Inorganic Chemistry*; Flint, C. D., Ed.; Kluwer Academic Publishers: Dordrecht, 1989; p 53.
(93) Our definitions of r_{ge}^{c} and r_{DA} are basically empirical, not theoretical: the r_{DA} parameter is determined from X-ray structural studies and r_{ge}^{c} is a parameter required by the experimental relationship between $E_{1/2}(\text{obsd})$ and $h\nu_{\text{DA}}$. For theoretical definitions of the distance parameters see refs 2, 28, 29, and 49.
(94) There is appreciable overlap of the solvation environments of donor and acceptor in the CN⁻-bridged complexes; for example, for the complexes with polypyridyl nonbridging ligands, the external radii of the D and A centers are about 6.5 and 3 Å for M(bpy)₂ and Ru(NH₃)₅, respectively, but $r_{\text{DA}} = 5.2$ Å.
(95) The assumption that a contribution of about 42 mV arises from such excited-state charge delocalization, rather than from solvational corrections for differences in charge, would also very nearly account for the relatively small value of $E_{1/2}(\text{Ru}(\text{NH}_3)_5^{3+,2+})$ in the (tpy)(bpy)Ru(CNRu(NH₃)₅)³⁺ complex. Owing to the uncertainty of this "correction", we have not included this point in Figure 10b.
(96) Richardson, D. E.; Sharpe, P. *Inorg. Chem.* **1993**, *32*, 1809.
(97) As a reviewer has noted, the values of H_{DA} inferred for $d\sigma/d\pi$ systems are larger than expected, on the basis of the expected σ/π orthogonality. However, we have already drawn attention to related features in the LMCT spectra of M(NH₃)₅Br²⁺ complexes,⁷⁰ and relatively few M–CN bonds are sufficiently linear⁹⁸ that the orthogonality relations would be rigorously applicable.
(98) See footnote 41 of Lessard, R. B.; Heeg, M. J.; Buranda, T.; Perkovic, M. W.; Schwarz, C. L.; Rudong, Y.; Endicott, J. F. *Inorg. Chem.* **1992**, *31*, 3091.
(99) Marcus, R. A. *J. Phys. Chem.* **1989**, *93*, 3078.